

\*Work performed under the auspices of the U. S. Atomic Energy Commission.

<sup>1</sup>Nicholas Nucker, Z. Phys. **227**, 152 (1969).

<sup>2</sup>W. Dilg and H. Vonach, Z. Naturforsch. **A26**, 442 (1971).

<sup>3</sup>L. Koester, private communication.

<sup>4</sup>V. E. Krohn and G. R. Ringo, Phys. Rev. **148**, 1303 (1966).

<sup>5</sup>E. Fermi and L. Marshall, Phys. Rev. **72**, 1139 (1947).

<sup>6</sup>L. L. Foldy, Phys. Rev. **83**, 688 (1951); Rev. Mod. Phys. **30**, 471 (1958).

<sup>7</sup>W. Dilg, L. Koester, and W. Nistler, Phys. Lett. **36B**, 208 (1971).

<sup>8</sup>L. Koester, private communication.

<sup>9</sup>J. H. Burns, P. A. Agron, and H. A. Levy, in *Noble Gas Compounds*, edited by H. H. Hyman (Univ. Chicago Press, Chicago, 1963), p. 211.

<sup>10</sup>M. F. Crouch, V. E. Krohn, and G. R. Ringo, Phys. Rev. **102**, 1321 (1956).

<sup>11</sup>A. D. MacQuillan, Proc. R. Soc. Lond. **A204**, 309 (1950).

<sup>12</sup>Yu. A. Alexandrov, R. P. Ozerov, and N. V. Ranev, Zh. Eksp. Teor. Fiz. Pis'ma Red. **15**, 398 (1972) [JETP Lett. **15**, 280 (1972)]; Yu. A. Alexandrov and V. K. Ignatovich, Joint Institute of Nuclear Research Report No. E3-6294, 1972 (unpublished).

<sup>13</sup>C. G. Shull, private communication.

PHYSICAL REVIEW D

VOLUME 8, NUMBER 5

1 SEPTEMBER 1973

## Experimental Study of the Rare $K^+$ Decay Modes: $K^+ \rightarrow \pi^+ \pi^0 \gamma$ , $K^+ \rightarrow \mu^+ \pi^0 \nu \gamma$ , $K^+ \rightarrow \pi^+ \gamma \gamma$ , $K^+ \rightarrow \pi^+ \nu \bar{\nu}$ , $K^+ \rightarrow \pi^0 \pi^0 e^+ \nu$ , and $K^+ \rightarrow e^+ \pi^0 \nu \gamma^*$

D. Ljung† and D. Cline

*Physics Department, University of Wisconsin, Madison, Wisconsin 53706*

(Received 22 January 1973)

Six rare stopped- $K^+$  decays have been studied in the 40-inch heavy-liquid bubble chamber at Argonne National Laboratory. The chamber was filled with  $\text{CF}_3\text{Br}$ . Twenty-two radiative  $K_{\pi_2}$  events with three converted  $\gamma$  rays were analyzed. The experiment was sensitive to positive pions with kinetic energy 55 to 102 MeV. The strengths ( $\gamma$  and  $\beta$ ) of the direct processes in the decay were determined to be  $\gamma = -0.02_{-0.43}^{+0.17}$ ,  $\beta = 0.0 \pm 0.3$ , and the branching ratio is  $(1.5_{-0.6}^{+1.1}) \times 10^{-4}$  for  $55 < T_{\pi^+} < 80$  MeV. These results are consistent with assuming the decay is dominated by internal bremsstrahlung. No events were found in the search for  $K^+ \rightarrow \mu^+ \pi^0 \nu \gamma$ , and the upper limit on the branching ratio is reported as  $6.1 \times 10^{-5}$  for  $\gamma$  energies greater than 30 MeV. No examples of the  $K^+ \rightarrow \pi^+ \gamma \gamma$  decay mode were found. The experiment was sensitive to pions with kinetic energy 6 to 102 and 114 to 127 MeV. The null result allowed us to discard several theoretical models which made branching-ratio predictions for this decay. Assuming a phase-space model for the pion spectrum, the upper limit is  $3.5 \times 10^{-5}$ . The upper limit on the neutral current decay  $K^+ \rightarrow \pi^+ \nu \bar{\nu}$  is reported as  $5.7 \times 10^{-5}$  assuming a vector interaction. The decay  $K^+ \rightarrow \pi^0 \pi^0 e^+ \nu$  was observed for the first time. Two events were found in which all four converted  $\gamma$ 's were seen. These two events give a branching ratio of  $(1.8_{-0.6}^{+2.4}) \times 10^{-5}$  for this decay. The form factor  $f_1$  for the decay is  $|f_1| = 0.97_{-0.19}^{+0.50}$ . These results are in good agreement with  $\Delta I = \frac{1}{2}$  rule predictions. Seventeen  $K^+ \rightarrow e^+ \pi^0 \nu \gamma$  events were observed. The branching ratio is reported as  $\Gamma(K^+ \rightarrow e^+ \pi^0 \nu \gamma) / \Gamma(K^+ \rightarrow e^+ \pi^0 \nu) = (0.48 \pm 0.20) \times 10^{-2}$  for  $E_\gamma > 30$  MeV and  $\cos \theta_{e\gamma} < 0.9$ .

### I. INTRODUCTION

This paper presents the final results and details of a bubble-chamber study of six of the rare decay modes of the  $K^+$  meson. Preliminary results have been published previously.<sup>1-3</sup> The decays studied (listed in order reported on in this paper) were  $K^+ \rightarrow \pi^+ \pi^0 \gamma$ ,  $K^+ \rightarrow \mu^+ \pi^0 \nu \gamma$ ,  $K^+ \rightarrow \pi^+ \gamma \gamma$ ,  $K^+ \rightarrow \pi^+ \nu \bar{\nu}$ ,  $K^+ \rightarrow \pi^0 \pi^0 e^+ \nu (K_{e\pi^0})$ , and  $K^+ \rightarrow e^+ \pi^0 \nu \gamma$ . The experiment was done in a heavy-liquid bubble chamber in which the  $\gamma$  conversion efficiency was high. Thus, rare  $K^+$  decays that had  $\pi^0$ 's or  $\gamma$ 's as final-state products were chosen to be studied

(or, as in the case of  $K^+ \rightarrow \pi^+ \nu \bar{\nu}$ , those decays in which the absence of  $\gamma$ 's was important).

The physics involved was the study of basic weak-interaction assumptions, the determination of form factors, and the testing of theoretical models. Thus, for example, the search for  $K^+ \rightarrow \pi^+ \nu \bar{\nu}$  tested the validity of the no-neutral-current rule, the radiative  $K_{\pi_2}$  study determined the form factors  $\gamma$  and  $\beta$ , and the search for  $K^+ \rightarrow \pi^+ \gamma \gamma$  was able to test and discard several theoretical models.

The experiment has had several significant results. The decay  $K^+ \rightarrow \pi^0 \pi^0 e^+ \nu$  was observed for

the first time. The first study of radiative  $K_{\mu 3}$  was made. The entire pion spectrum (except for the  $K_{\pi 2}$  region) for the decays  $K^+ \rightarrow \pi^+ \gamma \gamma$  and  $K^+ \rightarrow \pi^+ \nu \bar{\nu}$  was studied. The study of the lower end of the pion spectrum is particularly important in  $K^+ \rightarrow \pi^+ \gamma \gamma$  because many theoretical models predict that most events will occur in this region. Finally, results consistent with other recent experiments on radiative  $K_{\pi 2}$  and radiative  $K_{e 3}$  were obtained.

Section II of this paper discusses the experimental procedures common to the entire experiment. Sections III through VIII each present the details of the study of one of the six decay modes.

## II. EXPERIMENTAL PROCEDURES

### A. Beam and Bubble Chamber

This experiment was originally proposed in February, 1966, and the film was obtained in four separate runs at Argonne National Laboratory over a period of three years. The  $K^+$  particles were transported at 800–850 MeV/c by the 28° separated beam at the Zero Gradient Synchrotron (ZGS). The beam was degraded to approximately 500 MeV/c before entering the chamber in order to ensure that the  $K^+$  particles would stop in the chamber. The pion contamination of the beam was about 20%, and about 20% of the  $K^+$  particles decay in flight. For the first runs there was an average of seven beam tracks per picture, and for later runs the intensity was increased to 12 beam tracks per picture.

The Michigan 40-inch heavy-liquid bubble chamber was filled with heavy freon ( $\text{CF}_3\text{Br}$ ). Heavy freon was chosen for its short radiation length. Its 11 cm radiation length meant that most of the  $\gamma$ 's from  $K^+$  decays would convert in the chamber. The chamber was in a 46-kG magnetic field. For economy reasons the bubble-chamber cameras were switched during the experiment. The first 40% of the  $K^+$  decays studied is on 70-mm film, while the rest is on 35-mm film.

### B. Scanning

Figure 1 shows the scanning topologies for rare events. The following definitions and instructions were used by the scanners throughout the experiment to classify events. Only stopped- $K^+$  decays in an appropriate fiducial volume were considered. A stopped  $K^+$  was identified primarily by its ionization. The last few centimeters were required to be mostly solid, that is, so that individual bubbles could not be made out. Secondaries were classified as follows:

$\pi$ . The secondary stops and decays with a visible

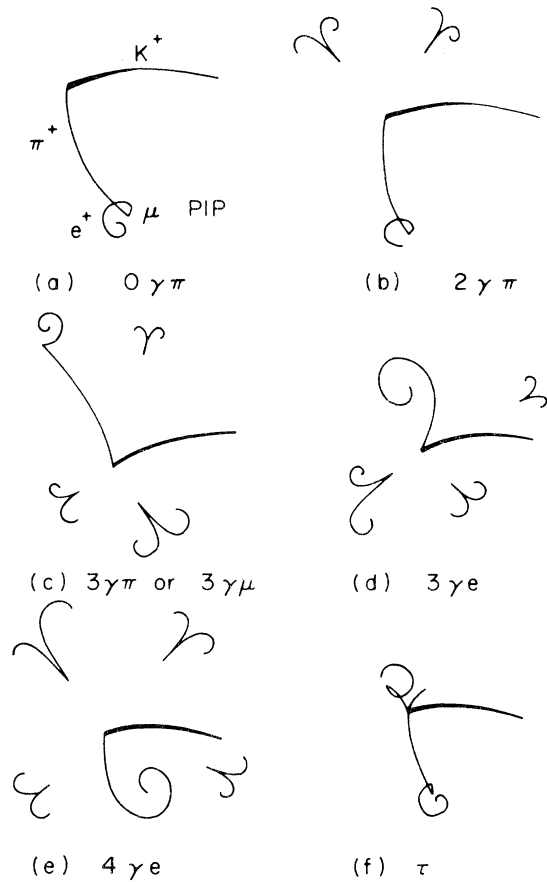


FIG. 1. Scanning topologies for rare events. Also included is the  $\tau$  decay used for normalization. The topologies are for the following decays: (a)  $K^+ \rightarrow \pi^+ \nu \bar{\nu}$ , (b)  $K^+ \rightarrow \pi^+ \gamma \gamma$ , (c)  $K^+ \rightarrow \pi^+ \pi^0 \gamma$  and  $K^+ \rightarrow \mu^+ \pi^0 \nu \gamma$ , (d)  $K^+ \rightarrow e^+ \pi^0 \nu \gamma$ , (e)  $K^+ \rightarrow \pi^0 \pi^0 e^+ \nu$ , (f)  $K^+ \rightarrow \pi^+ \pi^+ \pi^-$ .

$\mu$  pip. A  $\mu$  pip is the very short (less than one mm) muon track in the  $\pi$ - $\mu$ - $e$  decay chain. It is so called because it appears as a little pip between the pion and electron tracks. Also, to be classified as a  $\pi$ , the secondary must not scatter or interact.

$\mu$ . The secondary stops and decays, but no  $\mu$  pip is visible. Note that this definition includes most real muon secondaries plus the pion secondaries in which the  $\mu$  pip is obscured.

$e$ . The secondary is an electron and is identified by one or more of the following features: curvature, bremsstrahlung, knockon electrons, the lack of a secondary decay point, and/or the typical curling up of the track at the end of the secondary due to the magnetic field.

$K$  (Kinking). The secondary either has a large-angle scatter (greater than about 25°), interacts, or ends in a charge exchange. Most of these events are pions with a strong interaction, al-

though some are muons with large-angle Coulomb scatters. The fate of the original secondary after the scatter or interaction was not considered by the scanners.

*L* (Leaving). The secondary leaves the chamber.

$\tau$ . A stopped- $K^+$  decay with three charged secondaries; generally this event is  $K^+ \rightarrow \pi^+ \pi^+ \pi^-$ .

In addition to classifying the secondaries, the scanners also counted the number of  $\gamma$  rays pointing to the decay origin. No distinction was made among electron pairs, Compton electrons, and Dalitz pairs, and all are called  $\gamma$  rays. In this chamber with heavy freon, there is a large probability that an energetic electron (50 to 200 MeV/c) will lose a large portion of its energy (greater than 40 MeV/c) to a single photon, and then that this photon will convert in the chamber. Hence, a distinction was made between primary  $\gamma$ 's and bremsstrahlung  $\gamma$ 's. Primary  $\gamma$ 's ( $\gamma$ 's coming directly from the decay origin) were defined for the scanners as  $\gamma$ 's that did point to the origin but did not point as bremsstrahlung off of any electron track. The number of primary  $\gamma$ 's associated with any origin was noted by the scanners. Bremsstrahlung  $\gamma$ 's were defined as  $\gamma$ 's that pointed along a path tangential to an electron track. Bremsstrahlung is easily identifiable by the fact that it follows another  $\gamma$  or an electron secondary around in all views, always remaining in the same relative position. Bremsstrahlung  $\gamma$ 's were considered as such regardless of whether they also pointed directly to the origin. Thus, the scanners did not include bremsstrahlung in the count of  $\gamma$  rays associated with an event. It is necessary to eliminate bremsstrahlung  $\gamma$ 's in order to reduce the enormous background for the rare decays. Except in the case of radiative  $K_{e3}$  decay (treated separately), very few real events are lost by assuming that if a  $\gamma$  can be considered bremsstrahlung, then it is bremsstrahlung.

Several different sets of scan instructions were used. In a typical scan the scanners would be instructed to look for a certain subset of events. Generally a template giving the projected range of the secondary on the scan table was used to select events. In this way secondaries from ordinary decays with a fixed range, such as  $K_{\pi 2}$  and  $K_{\mu 2}$ , or with a limited range, such as the  $\pi^+$  from  $\tau'$  decay, could be quickly eliminated. The events selected were written down on a scan sheet, and then sketches were made. These sketches were used for future measuring and editing.

During most of the scans the scanners were forced to self-check their scanning efficiency by filling out a scan check sheet. Typically this sheet was filled out every other day, and it contained the totals of all classes of events found by the

scanner since the last scan check. These totals were compared with standards previously set up and, if a scanner failed to achieve a certain standard, she was instructed to rescan her previous frames in such a way so as to improve her performance. Alternatively she was given a "correction sheet" to be used in scanning for the next scan check. The correction sheet closely monitored the event type she was having trouble with, and generally ensured that her future scanning would pass the standard for that event.

### C. Event Measurement and Analysis

The events were measured by an image-plane digitizer. The entire event was measured in three views, and typically five points per track were recorded for electrons and beam tracks, while 10 to 15 points per track were used for pion and muon secondaries. The program CAMADJ was used to obtain the optical transformations from measuring table space to ideal film plane space. Geometry reconstruction was done by SHAPE. The electron energy was obtained from curvature using the Behr-Mittner method,<sup>4</sup> with a modification as suggested by Harvey Ring.<sup>5</sup> Pion and muon momenta were obtained from range measurements. Typical errors in the reconstructed variables are 20% to 30% for  $\gamma$  energy, 2% for pion and muon momenta, two to three degrees for track azimuths, and five degrees for dip. SQUAW was used for kinematic fitting, and it gives a  $\chi^2$  for each fit hypothesis along with the fitted variables. The data from SHAPE and SQUAW were analyzed using the program ARROW and INDIAN.

### D. Total Stopped- $K^+$ Decays

For the pion and muon decays the number of stopped- $\tau$  decays in the fiducial volume was used to determine the number of total  $K^+$  decays in the scan. For the first part of the film  $\tau$  decays were counted in every frame, while later they were counted only every fiftieth frame. A rescan determined the  $\tau$  scanning efficiency to be 98.5%. A total of 134645 frames were scanned for pion and muon decays, and the  $\tau$  count for these frames gave a total of 542100 stopped- $K^+$  decays. As the scan for  $K^+ \rightarrow \pi^+ \nu \bar{\nu}$  was stopped early, this decay was scanned for in 367500 stopped- $K^+$  decays. The error in the  $K^+$  count is  $\pm 4\%$ .

### E. Electron Identification and Normalization for Electron Events

Electron secondaries are identified on the scan table by their curvature, by the fact that when they stop there are no decay products, and often by the

presence of converted  $e^+e^-$  pairs due to bremsstrahlung. They are distinguished from pion and muon secondaries because the ionization of a pion or muon track will definitely darken as the particle stops, and after the particle stops a decay-product particle will emerge, generally in a new direction. Hence, the pion and muon secondaries usually have a definite kink at their decay point. In the case of a pion track, one gets a  $\mu$  pip at the end, with the dark short muon track and then the minimum-ionizing electron track. A muon will of course decay directly into a minimum-ionizing electron. Thus, an electron track is distinguishable from those of pions and muons by the fact that it remains minimum-ionizing until the very end, at which point it is obviously an electron track due to its small radius of curvature. Also, with the exception of bremsstrahlung, an electron track should not have large-angle kinks. Bremsstrahlung scatters are usually distinguishable from a stopped-secondary decay by the fact that there is no noticeable change in ionization from bremsstrahlung. Bremsstrahlung scatters are also usually forward, and one often sees the converted-bremsstrahlung  $e^+e^-$  pair.

Not all electron tracks are easily identifiable on the scan table, however. Steep electron tracks are usually not picked up by the scanners. The curvature of a steep track is not very helpful for identification (note that a track going straight up or down along the magnetic field lines is not deflected by the magnetic field), and also the ionization is hard to judge since most steep tracks appear dark. Thus, it is difficult, if not impossible, to separate steep electron tracks from steep pion and muon tracks. About 20% of all electron events are lost because the tracks are steep and unidentifiable. Further hindering electron identification is the fact that a pion or muon track can have some electron characteristics if the  $\pi-\mu-e$  or  $\mu-e$  decay chain has no large-angle kinks and if ionization information is poor.

The branching ratio of the rare electron decays is calculated relative to the  $K_{e3}$  branching ratio. The number of  $K_{e3}$  decays was obtained in the following manner. In the electron scans all electron secondaries regardless of number of associated  $\gamma$ 's were marked down. A total of 157890 frames containing 27506 electrons were scanned. As mentioned above there can be an ambiguity between electron secondaries and pion or muon secondaries. Both the rare electron candidates and a sample of the above 27506 secondaries were edited by a physicist in order to remove events in which this ambiguity could not be resolved. It was found that 83% (22952) of the secondaries marked down by the scanners were valid electron secondaries.

Only 6% of these valid electrons were borderline cases, in which the secondary was most likely an electron, even though it has some pion or muon characteristics. In the  $K_{e4}$  experiment it was found necessary to be absolutely certain of the electron identification and so for that experiment the editing was made stringent enough to exclude the 6% of borderline cases. The valid electron secondaries were assumed to come from  $K_{e3}$  decays, and the total valid electron secondaries were used in calculating electron branching ratios. The error in the number of valid electrons is 2.4%. From the  $\tau$  count for the pion and muon decays, it was found that the valid electrons represented 70% of the  $K_{e3}$  decays expected in the film.

#### F. Pion Identification by $\mu$ Pips

Three of the decays studied have a charged-pion secondary. For two of these decays,  $K^+ \rightarrow \pi^+\nu\bar{\nu}$  and  $K^+ \rightarrow \pi^+\gamma\gamma$ , it is necessary to identify the pion on the scan table in order to separate the desired decays from the background with muon secondaries. Pion identification was provided by observation of the  $\mu$  pip in the  $\pi-\mu-e$  decay chain. There are several problems in using this method of pion identification. In heavy freon the muon from a stopped-pion decay will decay after traveling less than 1 mm. Further hindering the detection of  $\mu$  pips is the fact that all tracks appear somewhat wobbly due to multiple scattering. Also the chamber is far from clean and extra bubbles appear throughout the chamber. All of these conditions mean that it is very hard to say what is and what is not a  $\mu$  pip. Depending on the criteria used, the percentage of  $\mu$  pips seen in a given sample of pions can vary from 35% to 75%. After studying both real  $\mu$  pips from pions and fake  $\mu$  pips from muons, the following criteria were chosen. First, the  $\mu$  pip must be definitely seen in at least two of the four 70-mm views. In the 35-mm film, because it only has three views, this requirement was relaxed so that a  $\mu$  pip must definitely be seen in at least one view plus "probably" be seen in a second view. Second, the editor must be able to follow the  $\pi-\mu-e$  chain. This eliminates any dark blobs that might be  $\mu$  pips. The breaks between  $\pi-\mu$  and  $\mu-e$  must be seen. Generally, this means the presence of two kinks, each greater than  $25^\circ$ . Virtually all the muons from  $\pi$  decays stop before decaying, and on our scanning tables, a  $\mu$  pip will appear to be about one millimeter long. Hence, any prospective  $\mu$  pips greater than one and a half millimeters were discarded.

The percentage of pions having a  $\mu$  pip as defined above was determined by looking at endings of the

two positively charged pion secondaries in  $\tau$  decays. The endings were classified into five categories. Pion secondaries less than 2 mm long were called "collinear" and discarded because the length of the pion was comparable to or less than the length of the  $\mu$  pip being searched for. Also discarded were endings that could not be seen because they became entangled in other parts of the  $\tau$  decay. These categories had to be discarded to eliminate problems common to  $\tau$  decay endings but virtually nonexistent for the decays being studied. Finally, any pions ending in a strong interaction were discarded because nuclear interactions are treated separately. About 10% of the endings were discarded in these three categories. The remaining endings were classified by a physicist as either having a  $\mu$  pip or not.  $\tau$ 's from all parts of the film were looked at, and the testing was spread out over the entire three-year period in which editing was done. To test the editor's consistency, some of the  $\tau$  endings looked at early in the experiment were classified a second time by the editor. In most cases the agreement on individual endings was exact. The result was that  $(53.1 \pm 3.4)\%$  of the pion endings were edited as having a  $\mu$  pip.

The scanner's efficiencies for selecting those events that the editor labeled as having a  $\mu$  pip were determined by having the scanners also look at  $\tau$  endings. The scanning efficiency for  $\mu$  pips varied between (71.3 and 88.6%) (plus or minus 5%) depending on the film and the scan.

One of the problems hindering pion identification is that muon secondaries can fake a  $\mu$  pip in several ways. There is a small chance that the  $\mu$  will scatter electromagnetically at the end of its range. The electron from the  $\mu$  decay can have a kink near the origin, usually due to bremsstrahlung. If one has a loose definition of  $\mu$  pips, then just the relatively poor track quality produced in heavy freon will cause one to see  $\mu$  pips where there is really nothing more than a widening of the track.  $K_{\mu 2}$  decays provide a clean sample of muon secondaries, and from a study of  $K_{\mu 2}$  ending it was determined that 1% of muon endings will be edited as having a fake  $\mu$  pip. At this low level there was no trouble with fake  $\mu$  pips.

#### G. Pions and Strong Interactions

Pions with strong interactions were discarded since the pion's range is usually changed by an interaction and thus the momentum by range is invalid. A strong-interaction event was labeled  $K$  (kink) by the scanners and was defined as a secondary that had a single large-angle scatter (generally greater than  $25^\circ$ ), or that ended in a multi-

prong star, or that ended in charge exchange. Also, the editor classified events having a definite and drastic change in ionization as having a strong interaction, even if no change in direction was apparent.

To determine the percentage of real events lost by discarding strong-interaction events, pions from  $K_{\pi 2}$  decays were studied. A physicist very carefully scanned 225 frames of 70-mm film. This short scan was used to determine several parameters. In this scan 70 events with a strong interaction were found in a sample of 174  $K_{\pi 2}$  decays. Thus,  $(40.2 \pm 4.8)\%$  of the pion secondaries from stopped- $K_{\pi 2}$  decays have a strong interaction.

In order to determine the percentage of secondaries having a strong interaction as a function of the secondaries' range, the distribution of strong interactions along the length of the 70  $K_{\pi 2}$  secondaries was obtained. Figure 2 shows this distribution, and Fig. 3 shows the percentage of pion secondaries having a strong interaction as a function of range as calculated from the distribution in Fig. 2. The dashed part of the curve above the  $K_{\pi 2}$  range is an extrapolation out to the maximum range possible for a pion secondary.

#### H. Leaving Tracks

All events with secondaries leaving the chamber were discarded from further consideration. The percentage of  $K_{\pi 2}$  and  $K_{\mu 2}$  events that leave was experimentally determined from the physicist scan. For the  $K_{\pi 2}$  events the sample used was composed of the  $K_{\pi 2}$  secondaries that did not have a strong interaction. Thus, the result is applicable to muons as well as to pions. The results are that  $(39.1 \pm 2.9)\%$  (181 out of 463) of the  $K_{\mu 2}$  decays leave the chamber and that  $(11.5 \pm 3.3)\%$  (12 out of 104) of the noninteracting  $K_{\pi 2}$  decays

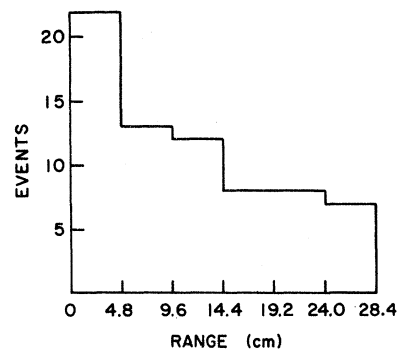


FIG. 2. 70  $K_{\pi 2}$  pion secondaries with a strong interaction. The abscissa is the distance along the pion from the  $K^+$  decay origin to the strong interaction.

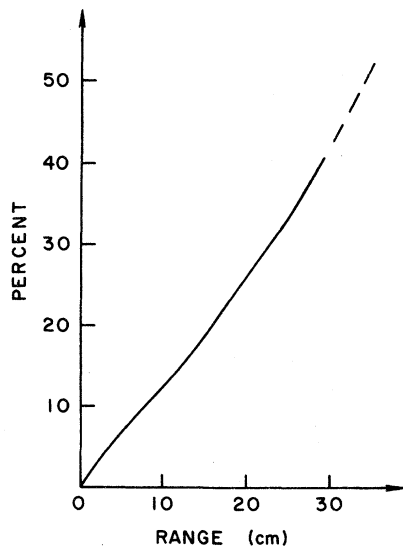


FIG. 3. Percentage of  $\pi$  secondaries having a strong interaction as a function of range.

leave. In order to determine the percentage leaving for ranges other than 28.9 cm ( $K_{\pi 2}$ ) and 51.2 cm ( $K_{\mu 2}$ ), the distance traveled before leaving the chamber was measured for a sample of leaving events. The results are shown in Fig. 4. Figure 5 shows the results of using the data of Fig. 4 to calculate the percentage of leaving tracks as a function of range. The solid line is a fit by hand made to follow the  $K_{\pi 2}$  data for shorter ranges and the  $K_{\mu 2}$  data at the longer ranges.

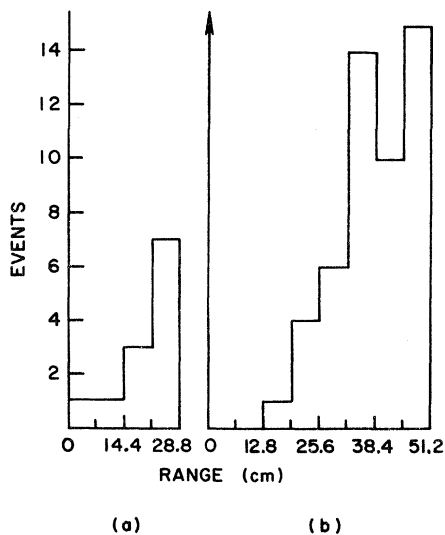


FIG. 4. Distance secondary travels before leaving chamber. (a) 12  $K_{\pi 2}$  events that leave chamber, (b) 50  $K_{\mu 2}$  events.

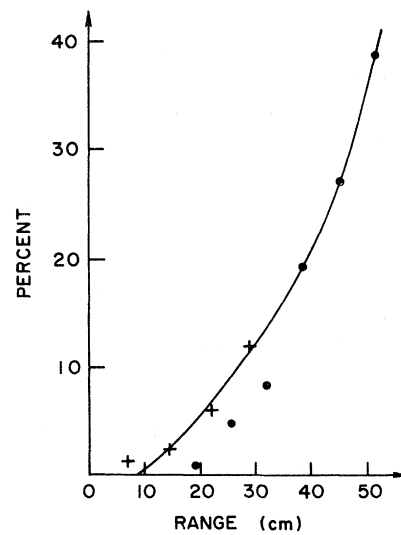


FIG. 5. Percentage of secondaries leaving chamber as a function of range.  $\bullet$  is a data point from the  $K_{\mu 2}$  events and + is a data point from the  $K_{\pi 2}$  events.

#### I. Range Cuts

At several stages throughout the experiment the common  $K_{\pi 2}$ ,  $K_{\mu 2}$ , and  $\tau'$  decays were discarded by making range cuts (on pion and muon secondaries). The effect of these cuts on the spectrum of rare decays being searched for must be considered. The first cut was made by the scanners by measuring the projected range of the pion or muon secondary being considered. All views were looked at, and the view in which the projected range was longest was used. The range of the  $\pi^+$  in  $K_{\pi 2}$  decays is 28.9 cm, and all events with projected ranges between 24.8 cm and 33.0 cm were discarded. This cut eliminated approximately 85% of the  $K_{\pi 2}$  decays remaining after eliminating leaving and strongly interacting tracks. The  $K_{\mu 2}$  range is 51.2 cm and 89% of the nonleaving  $K_{\mu 2}$  decays were eliminated by discarding all events with a projected range greater than 44.3 cm. Finally, the maximum range of the charged pion in a  $\tau'$  decay is 9.6 cm, and so most three  $\gamma$   $\tau'$  decays were separated from three  $\gamma$  radiative decays by eliminating three  $\gamma$  events with a projected range less than 7.4 cm. Note that this  $\tau'$  cut was not applied to  $0\gamma$  or  $2\gamma$  events. After this first stage, most remaining  $K_{\pi 2}$  and  $K_{\mu 2}$  decays are steep events that have relatively short projected ranges.

The second series of range cuts was made between scanning and measuring. The measuring tables can be used on line with a simple two-view reconstruction program to obtain an estimate of the range, dip, and depth of a single track. This

program, RANGER, gives the range to within 10%, and for approximately one half of the experiment RANGER measurements were made on all of the pion and muon events selected by the scanners. Events between 26.0 and 32.0 cm, events greater than 46.0 cm, and three  $\gamma$  events less than 8.5 cm were then eliminated. In this way most of the  $K_{\pi^2}$ 's,  $K_{\mu^2}$ 's, and  $\tau$ 's that survived the projected range cut were discarded. This step was dropped when it was decided to do no editing of the events before the full measurement.

The final cut was made after the entire event was measured and reconstructed using the program SHAPE. All remaining events with ranges between 26.0 and 31.0 cm, ranges greater than 44.0 cm, or three  $\gamma$  events with ranges less than 10.9 cm were discarded. Also, since very short pion tracks are not unambiguously identifiable as pions, a cutoff at 0.2 cm was made for pion tracks associated with  $0\gamma$ 's or  $2\gamma$ 's. Actually, only the final series of cuts is needed to virtually eliminate all stopped, nonleaving, noninteracting  $K_{\pi^2}$ ,  $K_{\mu^2}$ , and  $\tau$ ' decays as a source of background. The first two cruder cuts are used to speed up the scanning and to reduce the amount of measuring.

To study the effect of these cuts on the rare decays, a sample of  $K_{\pi^2}$  and  $K_{\mu^2}$  decays was measured using all three methods: projected range, RANGER, and full event measurement. The range distributions obtained for these fixed momenta decays were then scaled to other ranges and used to determine the percentage of events surviving all three cuts as a function of range. The results are presented in Fig. 6. The vertical lines in the figure are due to the relatively sharp final cut. The rounding off of the corners is almost entirely due to the projected range cut, as it is the least accurate.

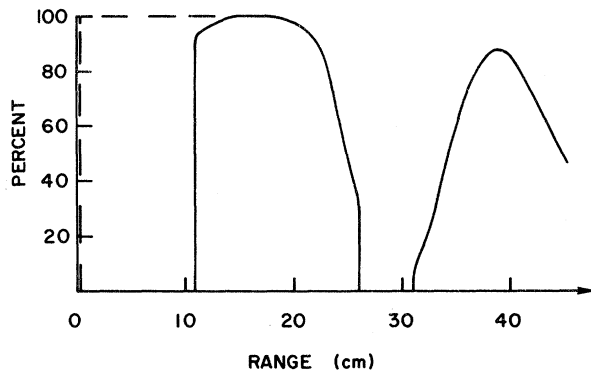


FIG. 6. Percentage of secondaries passing range cutoffs as a function of range. Below 14 cm of range, the solid line is for  $3\gamma$  events and the dashed line is for  $0\gamma$  and  $2\gamma$  events.

#### J. Scanners' Pion and Muon Detection Efficiency

The scanners' efficiency for finding and properly marking down an event that has a pion or muon secondary with a range from a couple of millimeters to 45 cm (excluding  $K_{\mu^2}$  secondaries) was determined to be  $(80 \pm 10)\%$ . Events lost due to one of the following scanner errors were considered: missing the event entirely, incorrect measurement of projected range, incorrect labeling of a secondary as having a strong interaction or as leaving, and finally labeling a pion or muon secondary as an electron. All of these errors cause the event to be lost from further consideration and hence they are treated together. Notice that this efficiency does not consider  $\gamma$  numbering errors or  $\mu$  pip labeling errors as they are treated separately.

#### K. $\gamma$ Detection Probability

The  $\gamma$  detection probability is defined as the product of the  $\gamma$  conversion probability and the scanner's  $\gamma$  efficiency. The  $\gamma$  conversion probability is the probability that a  $\gamma$  will convert into an  $e^+e^-$  pair or produce a Compton electron before leaving the chamber. For any individual  $\gamma$  it is a function of the liquid in the chamber, the distance traveled in the chamber, and the energy of the  $\gamma$ . For this experiment the liquid is fixed and the  $\gamma$  conversion probability was averaged over all of the possible distances traveled. The energy dependence was specifically considered. The scanner's  $\gamma$  efficiency is the probability that a scanner will find and assign to the correct decay origin a  $\gamma$  that has converted in the chamber. Thus, the  $\gamma$  detection probability is the probability that a  $\gamma$  (or a set of  $\gamma$ 's, such as the two  $\gamma$ 's from a single  $\pi^0$  decay) will convert in the chamber and will be correctly labeled by the scanner.

The  $\gamma$  conversion probabilities were determined experimentally by studying some of the ordinary  $K^+$  decays. The results of the physicist scan, in which all converted  $\gamma$ 's were carefully assigned to the proper origin, were used. The  $2\gamma$  conversion probability (chance that both  $\gamma$ 's from a single  $\pi^0$  will convert) was determined to be  $(70.6 \pm 4)\%$ . Most of these  $\gamma$ 's come from  $K_{\pi^2}$  decays with  $\pi^0$  momentum equal to 205 MeV/c. Thus, this figure is valid for a  $\pi^0$  with momentum of approximately 200 MeV/c. The  $4\gamma$  conversion probability is needed for the study of  $K^+ \rightarrow \pi^0\pi^0e^+\nu$ . The average  $\pi^0$  momentum in this decay is assumed to lie between the  $\pi^0$  momentum for decays with a single  $\pi^0$  and the average  $\pi^0$  momentum in the decay  $K^+ \rightarrow \pi^+\pi^0\pi^0$ . Thus, the  $K_{e^4}$   $4\gamma$  conversion probability is expected to lie between 49.8% (square of the single  $\pi^0$

conversion) and 35.7% (experimental value found for the four  $\gamma$ 's from  $\tau'$  decays). A value of  $(43 \pm 5)\%$  is assumed.

The scanning efficiency for finding both  $\gamma$ 's from a  $\pi^0$  decay was found to be  $(84.5 \pm 2.2)\%$ . The scanning efficiency for finding three  $\gamma$ 's must consider an additional psychological factor. The radiative decays with three  $\gamma$ 's are all very similar to common decays that have only two  $\gamma$ 's. It is found that the scanning efficiency for the third (usually small)  $\gamma$  is much lower than the efficiency for finding the first two. A rescan of some of the  $3\gamma$  radiative  $K_{\pi_2}$  events showed that the scanning efficiency for finding all three converted  $\gamma$ 's is only  $(33 \pm 12)\%$ . This low efficiency indicates the scanners miss a large number of radiative events merely because they are conditioned to see two  $\gamma$ 's instead of three. The above efficiencies are for a single scan. In most cases the scanning efficiency was increased appropriately to account for rescans. In the case of radiative  $K_{\pi_2}$  and  $K_{e_4}$ , the scanning efficiency was assumed to be 100% because a physicist checked events with one  $\gamma$  less than the event topology being searched for. This check picked up  $\gamma$ 's that had been previously missed by the scanner.

The energy dependence of the conversion probability was determined by looking at the energy distribution of unconverted  $\gamma$ 's from  $K_{\pi_2}$  decays. A sample of  $K_{\pi_2}$  decays with only one  $\gamma$  was measured and fitted to  $K_{\pi_2}$ . The fitted energies of the missing  $\gamma$ 's for those events having a  $\chi^2$  less than 3.5 to the two-constraint fit are shown in Fig. 7(a). Note that more low-energy  $\gamma$ 's were

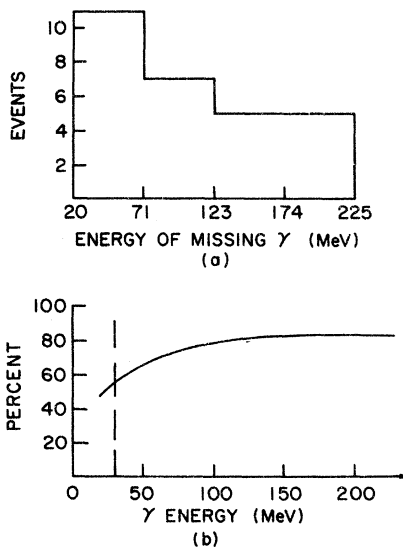


FIG. 7. (a) The fitted energy of the nonconverting  $\gamma$  for 28  $K_{\pi_2}$  events with only one  $\gamma$  pointing to the decay origin. (b)  $\gamma$  detection probability as a function of  $\gamma$  energy. The dashed line indicates the cut at 30 MeV.

missed than high-energy  $\gamma$ 's. The Barschall-Powell theorem says that the  $\gamma$ 's from a  $K_{\pi_2} \pi^0$  will have a flat energy distribution in the laboratory frame from 20 MeV to 225 MeV. Thus, Fig. 7(a) shows the skewing due to the energy dependence of the detection probability. Figure 7(b) shows the resulting single- $\gamma$  detection probability as a function of  $\gamma$  energy. It was calculated using the information in Fig. 7(a) along with information on conversion probabilities and scanning efficiencies. For simplicity, the energy dependence of missing a  $\gamma$  because the scanner fails to see it was assumed to be the same as that for failing to convert.

The information in this section was used to calculate the  $\gamma$  detection probability for each particular rare event. The energy dependence was accounted for by using the theoretical  $\gamma$  spectrum for each event and in some cases the  $\pi^0$  momentum spectrum. Thus, for example, in  $K^+ \rightarrow \pi^+ \pi^0 \gamma$  decays the radiative  $\gamma$  detection probability has the energy dependence shown in Fig. 7(b), while the  $\pi^0 (2\gamma)$  detection probability is assumed to vary as follows: for  $\pi^0$ 's up to 100 MeV/c it is assumed to be 50%, and from 100 to 200 MeV/c it increases linearly up to 60%.

### III. EXPERIMENTAL STUDY OF $K^+ \rightarrow \pi^+ \pi^0 \gamma$

#### A. Theoretical Review

The observation of a large direct emission process in the decay  $K^+ \rightarrow \pi^+ \pi^0 \gamma$  would have several interesting theoretical consequences, which warrant the experimental search for this process. Perhaps the most important among these consequences is the usefulness of the  $\pi\pi\gamma$  decay for investigating  $CP$  and  $T$  violation, which depends directly on the existence of an appreciable direct emission amplitude.<sup>6-8</sup> Furthermore, the electromagnetic contribution to the breaking of the  $\Delta T = \frac{1}{2}$  rule for  $K \rightarrow \pi\pi$  decays is likely related to the relative size of the direct and internal bremsstrahlung amplitudes in  $K \rightarrow \pi\pi\gamma$  decay.<sup>9</sup>

Theoretically, the decay  $K^+ \rightarrow \pi^+ \pi^0 \gamma$  can proceed by either internal bremsstrahlung or else by some direct-emission process. Assuming that only the lowest-order multipoles contribute to the direct process, the differential decay rate can be written as<sup>9,10</sup>

$$\frac{d\Gamma}{dT_{\pi^+} d\cos\theta} = \alpha(K_{\pi_2}) \phi (I_b + \gamma I_{\text{int}} + \gamma^2 I_{E1} + \beta^2 I_{M1}),$$

where

$$T_{\pi^+} = \pi^+ \text{ kinetic energy,}$$

$$\cos\theta = \text{angle between } \pi^+ \text{ and extra } \gamma \text{ (non-}\pi^0\text{),}$$



$\alpha(K_{\pi_2}) = K_{\pi_2}$  branching ratio = 0.2092,

$\phi$  is the phase-space factor,  $I_b$  is the internal bremsstrahlung contribution,  $I_{E1}$  and  $I_{M1}$  are the  $E1$  and  $M1$  direct emission contributions, and  $I_{int}$  is the contribution from the interference between internal bremsstrahlung and the  $E1$  term.  $\gamma$  and  $\beta$  are form factors giving the strength of the  $E1$  and  $M1$  terms.

The purpose of an experiment is the determination of  $\gamma$  and  $\beta$ . These parameters can be obtained from a study of the pion spectrum and its correlation with the  $\cos\theta$  spectrum. The total branching ratio is also a function of  $\gamma$  and  $\beta$ . There are several theoretical calculations<sup>11</sup> of  $\gamma$  and  $\beta$ . These range from 0.04 to 0.45 for the absolute value of  $\gamma$  and from zero to one for the absolute value of  $\beta$ .

#### B. Selection of $K^+ \rightarrow \pi^+ \pi^0 \gamma$ Events

The scanners searched for a stopped- $K^+$  decay with three  $\gamma$ 's pointing to the origin. The secondary was required to have no large-angle scatters as well as a range below the  $K_{\pi_2}$  region and above the  $\tau'$  region. The secondary was classified as either a  $\mu$  (no  $\mu$  pip) or a  $\pi$  (with a visible  $\mu$  pip). A total of 542 100 stopped- $K^+$  decays were scanned. Four hundred and eighty candidates were measured, and after reconstruction and fitting, the following three cuts were applied to the candidates. Only events with a fit giving a  $\chi^2$  probability greater than 0.001 were accepted. Second, the difference between the measured  $\pi^+$  momentum as determined from range and the fitted  $\pi^+$  momentum was required to be less than 10.5 MeV/c, and third the fitted pion kinetic energy had to be in the range of 55 to 102 MeV. This cut on the fitted energy range corresponds to the cuts applied to the measured range of the secondary. Events surviving these cuts were carefully edited by a physicist in order to determine if the event satisfied the scanning criteria. 23 radiative  $K_{\pi_2}$  events were left for analysis.

In order to determine  $\cos\theta$ , the decision as to which of the three  $\gamma$ 's was the extra (non- $\pi^0$ )  $\gamma$  must be made. In some cases only one permutation made a successful  $K^+ \rightarrow \pi^+ \pi^0 \gamma$  fit. Many events had two choices, however, and for some events all three  $\gamma$ 's worked. The  $\gamma$  which gave the lowest average  $\chi^2$  for the  $K^+ \rightarrow \pi^+ \pi^0 \gamma$  fit when it was used as the extra  $\gamma$  was chosen as the extra  $\gamma$ . Unfortunately, there were six events in which two or three  $\gamma$ 's gave comparable (within 30%)  $\chi^2$ 's despite repeated measurement. In some of these cases it became evident that a clear-cut resolution of the ambiguity was beyond the experimental accuracy. Unfortunately, this ambiguity has a significant effect on the analysis of  $\gamma$  and  $\beta$ . As is discussed

later, the effects of possible incorrect  $\gamma$  assignment will be included in the errors.

Since the scanning efficiency for  $\gamma$ 's drops off rapidly for low-energy  $\gamma$ 's, a cutoff on  $\gamma$  energies was applied, and events were accepted only if the fitted energy for the extra  $\gamma$  was greater than 30 MeV. Figure 8 gives the experimental  $T_{\pi^+}$ ,  $\cos\theta$ , and energy of the extra  $\gamma$  spectra for the final sample of twenty-two events. The solid curves are the expected experimental spectra assuming  $\gamma = \beta = 0$  (internal bremsstrahlung only). In calculating the expected experimental spectra, the following experimental efficiencies (as discussed in Sec. II) were considered: the efficiencies for finding the  $\pi^+$  as a function of pion kinetic energy considering losses due to strong interactions, leaving secondaries, and range cuts; the  $\gamma$  detection probability for the extra  $\gamma$  as a function of its energy; and the  $\gamma$  detection probability for the two  $\gamma$ 's from the  $\pi^0$  as a function of the  $\pi^0$  momentum.

#### C. Background Discussion

It is expected that the events picked up in this experiment are relatively clean of background. The following three types of background will be discussed:  $2\gamma$  events with an accidental third  $\gamma$ , in flight  $K^+ \rightarrow \pi^+ \pi^0 \pi^0$  decays in which only three  $\gamma$ 's convert, and other rare  $K^+$  decays. An accidental  $\gamma$  can have its true origin either outside or inside

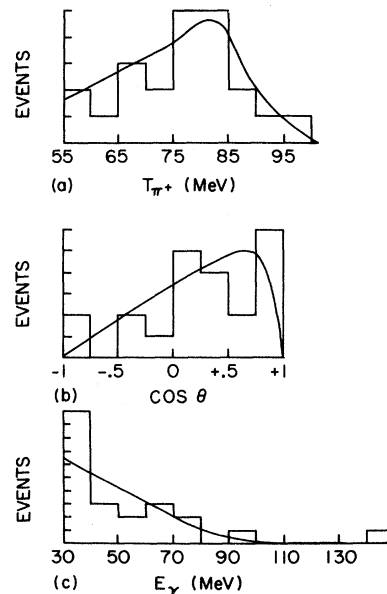


FIG. 8. Experimental spectra for 22  $K^+ \rightarrow \pi^+ \pi^0 \gamma$  events. The solid lines give expected experimental spectra for internal bremsstrahlung alone. (a) Kinetic energy of positive pion ( $T_{\pi^+}$ ), (b) cosine of the angle between the positive pion and the extra (non- $\pi^0$ )  $\gamma$  ( $\cos\theta$ ), (c) energy of the extra  $\gamma$  ( $E_\gamma$ ).

the bubble chamber. Background due to a  $2\gamma$  decay such as  $K_{\mu 3}$  plus an accidental  $\gamma$  originating within the chamber is eliminated by rather harsh editing of the  $\gamma$ 's. For all events the entire bubble chamber was searched for alternate origins for the three  $\gamma$ 's pointing to a possible  $K^+ \rightarrow \pi^+ \pi^0 \gamma$  decay vertex. In all cases where a possible alternate origin existed, the  $\gamma$  was associated with the origin to which it best pointed. If it pointed approximately as well to both origins and if it was reasonable to assume that the  $\gamma$  came from the alternate origin, it was assigned there. From a consideration of the number of ambiguous cases encountered in editing, it is expected that no more than 5 to 10% of the real events will be discarded by this requirement on the  $\gamma$ 's. An estimate of the number of background events due to accidentals originating outside of the chamber was made in the following manner. In a short scan by a physicist the number of  $\gamma$ 's with no apparent bubble chamber origin was counted. This number was used in a calculation of the number of accidental  $\gamma$ 's that would actually point to an origin and would cause a fake event to survive all cuts. The result was that less than one event was expected as background due to accidental  $\gamma$ 's originating from outside the chamber. Thus, accidental  $\gamma$ 's are not expected to produce background for radiative  $K_{\pi 2}$ . The editing was the same for the other rare decays and so the result also applies to them.

Conceivably a  $\tau'$  decay could be picked up if the  $K^+$  decayed in flight and the positive pion secondary went forward so that its range would be greater than the ordinary stopped- $\tau'$  decay limit. Apparently the chance that such a decay will indeed fit the  $K^+ \rightarrow \pi^+ \pi^0 \gamma$  hypothesis is small, since all of the 22 events were fitted to the three-vertex two-constraint  $\tau'$ -in-flight hypothesis and none of the events fit. This hypothesis gave acceptable fits when applied to events that were clearly examples of  $\tau'$ -in-flight decays. To check for contamination from stopped- $\tau'$  decays, those events near the  $\tau'$  end of the spectrum were fitted to the stopped- $\tau'$  hypothesis. None had acceptable fits. The only remaining way for a  $\tau'$  decay to become background is for an in-flight- $\tau'$  decay to have some accident (like a  $\pi^+$  scatter at the decay origin) such that it fails the  $\tau'$ -in-flight hypothesis but passes the radiative  $K_{\pi 2}$  hypothesis. This background is negligible just from simple calculations of the total number of in-flight- $\tau'$  decays one expects in the film plus some simple assumptions as to how often an undetected accident occurs.

Since the secondary is not required to have a  $\mu$  pip and hence is not positively identified as a pion, there is a chance that a radiative  $K_{\mu 3}$  decay could be accepted as a  $K^+ \rightarrow \pi^+ \pi^0 \gamma$  decay. However,

this background is expected to be small for the following reasons. In general, one would not expect a real radiative  $K_{\mu 3}$  decay, which is four-body and hence not coplanar, to be able to fit as a radiative  $K_{\pi 2}$  decay, which is three-body and coplanar. Also the branching ratio for radiative  $K_{\mu 3}$  is expected to be an order of magnitude lower than radiative  $K_{\pi 2}$ . Five of the 22 radiative  $K_{\pi 2}$  events do not have an identifiable  $\mu$  pip; one would expect, however, at least that many in an experiment of this type due to the radiative  $K_{\pi 2}$  events alone. Finally, for the branching-ratio calculation, only those events with  $\mu$  pips are used, and hence virtually any chance of this type of background is eliminated. Rare electron decays with three or more  $\gamma$ 's, such as radiative  $K_{e3}$  or  $K_{e4}$ , can be eliminated as a source of background simply because at this level the confusion between pion and electron secondaries is small. In conclusion, it is expected that the sample of radiative  $K_{\pi 2}$  events has no more than one background event from all sources.

#### D. Calculation of $\gamma$ and $\beta$

The experimental values of pion kinetic energy and  $\cos\theta$  were used in a maximum-likelihood analysis in order to determine  $\gamma$  and  $\beta$ . To study the effect of events with an ambiguity in the choice of the extra  $\gamma$ , many different runs of the likelihood program were made, each with a different possible set of choices of  $\cos\theta$  for the ambiguous events. It was found that the calculated value of  $\gamma$  varied from +0.15 to -0.45. Some of the ambiguous events had little effect on  $\gamma$  regardless of which  $\gamma$  was chosen as the extra one, while others caused drastic changes. Figure 9 shows the changes in the likelihood function (assuming  $\beta$  to equal zero) due to different choices for the extra  $\gamma$  for the event causing the largest fluctuations in the likelihood function. All three  $\gamma$ 's could be considered the extra  $\gamma$  for this event. Note the shifting in the relative importance of the two main peaks at 0.0 and -0.4 as the extra  $\gamma$  is changed. Since no particular set of extra  $\gamma$ 's was definitely favored over another, the maximum-likelihood results are a range for  $\gamma$  and  $\beta$ . The range is such that it includes all the values calculated from various reasonable permutations of the experimental data. Thus,

$$-0.45 < \gamma < +0.15 \text{ (assuming } \beta = 0 \text{) ,}$$

$$|\beta| < 0.3 \text{ (assuming } \gamma = 0 \text{) .}$$

A Monte Carlo study was done to determine the effect of ambiguous events and other experimental errors on the determination of  $\gamma$ . When ambiguous events were added to randomly generated radiative

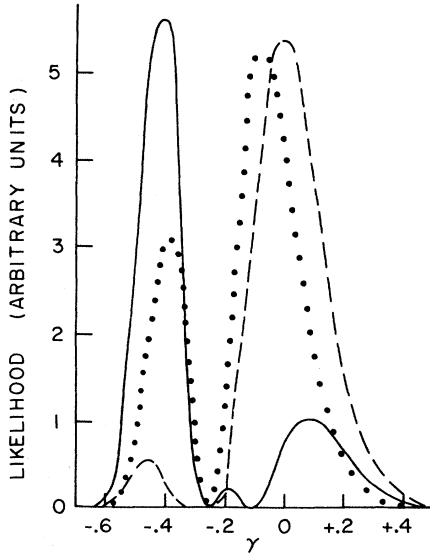


FIG. 9. Effect on likelihood function of a single ambiguous event. All three  $\gamma$ 's for this event can be considered the extra  $\gamma$ . The three different curves each correspond to a different choice for the extra  $\gamma$ .

$K_{\pi 2}$  events, it was found that the maximum-likelihood program often gave results with a double peak much like the actual experimental data. Thus, the importance of reducing this ambiguity in future experiments that attempt to determine  $\gamma$  and  $\beta$  is established.<sup>12</sup> The Monte Carlo study also showed that errors in the determination of experimental efficiencies on the order of the errors quoted in Sec. II only cause shifts in  $\gamma$  of a couple of hundredths.

#### E. $K^+ \rightarrow \pi^+ \pi^0 \gamma$ Branching Ratio

Since the branching ratio is a function of  $\gamma$  and  $\beta$ , its experimental determination can be used to improve the determination of  $\gamma$  and  $\beta$ . The calculation of the branching ratio used only those events with a  $\mu$  pip found in a section of film in which all  $2\gamma$  pion events (as well as  $3\gamma$  events) were analyzed for radiative  $K_{\pi 2}$  events. These two  $\gamma$  events were edited by a physicist who looked for any third  $\gamma$ 's that may have been missed by the scanners. This film was also rescanned and the combined scanning efficiency for finding three converted  $\gamma$ 's was assumed to be 100%. The branching ratio was calculated for three pion kinetic energy ranges and the results are given below (note the ranges overlap). In each range the total experimental efficiency for finding  $K^+ \rightarrow \pi^+ \pi^0 \gamma$  events was calculated. For efficiencies due to losses that depend on the pion kinetic energy (such as losses due to strong interactions, range cuts, and leaving tracks), the internal bremsstrahlung spectrum was assumed. A 10% loss was assumed due to editing and process-

ing events. The resulting total efficiencies were 18.0%, 13.9%, and 6.0% for the respective ranges:

Pion kinetic-energy range ( $T_{\pi^+}$ )	Experimental branching ratio	Theoretical branching ratio for internal bremsstrahlung
55-80 MeV	$(1.5_{-0.6}^{+1.1}) \times 10^{-4}$	$1.39 \times 10^{-4}$
55-90 MeV	$(2.6_{-1.1}^{+1.5}) \times 10^{-4}$	$2.72 \times 10^{-4}$
55-102 MeV	$(6.8_{-2.1}^{+3.7}) \times 10^{-4}$	$6.87 \times 10^{-4}$

The quoted errors (68% confidence level) are due largely to the Poisson distribution for the number of events, but they also include all the errors in the various experimental efficiencies. Note the excellent agreement between the experimental values and those predicted assuming only internal bremsstrahlung ( $\gamma = \beta = 0$ ). The branching ratio was used to calculate  $\gamma$  and  $\beta$ , and the results were combined with the results of the maximum-likelihood analysis of the  $T_{\pi^+}$ ,  $\cos\theta$  spectra. The final experimental determination of  $\gamma$  and  $\beta$  from this experiment is

$$\begin{aligned} \gamma &= -0.02_{-0.43}^{+0.17}, \\ \beta &= 0.0 \pm 0.3. \end{aligned}$$

Several other experiments have determined  $\gamma$  and  $\beta$ . The statistics and results of most of these studies are similar to those of this experiment, with the exception of a recent high-statistics result of Abrams *et al.*<sup>13</sup> Excluding the Abrams result, the experimental data can be combined by multiplying all the likelihood functions together. A "floor" on each separate experiment of 1% of that experiment's maximum likelihood is assumed, so that a minimum of one experiment does not completely overwhelm all other data at that point. The results for  $\gamma$  and  $\beta$  are shown in Fig. 10. From this figure one obtains approximately

$$\begin{aligned} \gamma &= 0.1 \pm 0.1, \\ |\beta| &= 0.15_{-0.15}^{+0.10}. \end{aligned}$$

## IV. SEARCH FOR RADIATIVE $K_{\mu 3}$ DECAYS

### A. Theoretical Review

Fischbach and Smith<sup>14</sup> have theoretically studied the decay  $K^+ \rightarrow \mu^+ \pi^0 \nu \gamma$  including both internal-bremsstrahlung contributions and structure-dependent terms. Theoretically, with a large number of these decays the  $K_{13}$  form factors could be determined. Experimentally, however, it would be difficult to extract this information as the structure-dependent terms are expected to be small and

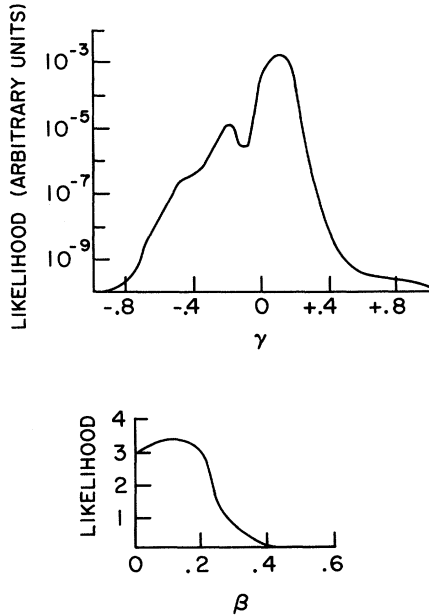


FIG. 10. Product of all experimental likelihood functions for determination of  $\gamma$  and  $\beta$ .

also the decay is hard to identify positively. Assuming reasonable values for the form factors the prediction of Fischbach and Smith for the branching ratio is

$$\frac{\Gamma(K^+ \rightarrow \mu^+ \pi^0 \nu \gamma, E_\gamma > 30 \text{ MeV})}{\Gamma(K^+ \rightarrow \mu^+ \pi^0 \nu)} = 0.70 \times 10^{-3}.$$

#### B. Selection of Candidates and Background Discussion

The events selected for the radiative  $K_{\pi 2}$  experiment were also considered as radiative  $K_{\mu 3}$  candidates. Also events with ranges above the  $K_{\pi 2}$  region were considered. After geometric reconstruction and kinematic fitting, several cuts were applied to these candidates. In order to be kept as a candidate an event was required to have a  $\chi^2$  probability for the two-constraint two-vertex fit to  $K_{\mu 3} + \gamma$  greater than 0.001. Also the fitted muon momentum was required to be either between 113.5 MeV/c and 168.5 MeV/c or between 182.7 MeV/c and up to the kinematic limit of 215 MeV/c. This cut along with the range cuts eliminated the common  $\tau'$  and  $K_{\pi 2}$  decays. Finally, since momentum by range could be measured quite accurately, the measured and fitted muon momentum had to agree within 10.5 MeV/c.

97 events survived these cuts and were edited by a physicist on the scan table. Primarily this editing was done to eliminate ordinary  $2\gamma$  decays that had been incorrectly assigned a third  $\gamma$ . Also at this time, secondaries that decayed in a visible  $\pi-\mu-e$  decay chain were eliminated as they could

be positively identified as being a pion. Only six events remained after editing.

All six of the remaining events also survived cuts similar to the above except applied to the decay<sup>15</sup>  $K^+ \rightarrow \pi^+ \pi^0 \gamma$ . Thus, the remaining background was due to radiative  $K_{\pi 2}$  decays, and a study was made of how to separate radiative  $K_{\pi 2}$  events from radiative  $K_{\mu 3}$  events. In the radiative  $K_{\pi 2}$  experiment, seventeen other events were found that were  $K^+ \rightarrow \pi^+ \pi^0 \gamma$  candidates. These 17 events were definitely radiative  $K_{\pi 2}$  events and not radiative  $K_{\mu 3}$  events because the secondary decayed with a visible  $\pi-\mu-e$  decay chain. However, when the  $\pi-\mu-e$  decay chain was neglected on these events and they were analyzed as radiative  $K_{\mu 3}$  decays, it was found that they fitted both radiative decays equally well. In general, these fake radiative  $K_{\mu 3}$  fits reconstructed a low-energy neutrino that tended to go along the muon direction. This is what would be expected from conservation of energy and momentum. Thus, it was found that all radiative  $K_{\pi 2}$  events can be expected to fit radiative  $K_{\mu 3}$ . However, the reverse would not be expected to be true. A real radiative  $K_{\mu 3}$  event is a four-body decay and usually would not fit a three-body coplanar decay such as radiative  $K_{\pi 2}$ . Thus, the final cut was to eliminate any events which passed the radiative  $K_{\pi 2}$  cuts. There were no  $K^+ \rightarrow \mu^+ \pi^0 \nu \gamma$  candidates left.

#### C. Upper Limit on $K^+ \rightarrow \mu^+ \pi^0 \nu \gamma$ Branching Ratio

In order to set an upper limit on the branching ratio, the efficiency for finding radiative  $K_{\mu 3}$  events was determined. The muon spectrum for  $K^+ \rightarrow \mu^+ \pi^0 \nu \gamma$  was assumed to be the same as for  $K^+ \rightarrow \mu^+ \pi^0 \nu$  and it was found that 51% of all real events would be accepted by the cuts on the muon momentum. The experimental efficiencies discussed in Sec. II were applied. For the extra  $\gamma$  detection efficiency the  $\gamma$  spectrum of Fischbach and Smith was used with an energy cutoff of 30 MeV on the extra  $\gamma$ . A study of how often lower-constraint fits such as radiative  $K_{\mu 3}$  would fake a fit to a higher-constraint fit such as radiative  $K_{\pi 2}$  indicated that only 5% of the real events would be lost due to discarding events that passed the radiative  $K_{\pi 2}$  cuts. The total efficiency was 7% and thus,

$$\frac{\Gamma(K^+ \rightarrow \mu^+ \pi^0 \nu \gamma, E_\gamma > 30 \text{ MeV})}{\Gamma(K^+ \rightarrow \text{all})} < 6.1 \times 10^{-5}$$

at the 90% confidence level. Finding a single event in this experiment would have corresponded to a branching ratio of  $2.7 \times 10^{-5}$ , which would have been compared with the Fischbach and Smith branching ratio<sup>16</sup> of  $2.2 \times 10^{-5}$ . Thus, the experimental result

is consistent with assuming that there are no unusually large structure-dependent terms.

## V. SEARCH FOR $K^+ \rightarrow \pi^+ \gamma \gamma$

### A. Theoretical Review

Observation of the decay  $K^+ \rightarrow \pi^+ \gamma \gamma$  would be of theoretical interest because it might shed some light on the mechanism responsible for the breaking of the  $\Delta I = \frac{1}{2}$  rule in the ordinary  $K_{\pi 2}$  decay. This experiment is the first one to search for this decay in the lower end of the pion spectrum. This region is important as several theoretical models of the decay have predicted that the majority of these decays will have pions with a kinetic energy below 60 MeV.

The decay  $K^+ \rightarrow \pi^+ \gamma \gamma$  is expected to exist as a result of first-order weak and second-order electromagnetic interactions. In principle the decay could proceed either by inner bremsstrahlung or else by direct emission of photons. However, it has been pointed out that the inner bremsstrahlung terms must vanish due to gauge invariance and the pseudoscalar nature of the mesons.<sup>17</sup> Various theoretical models have been used to estimate the contribution to the direct  $K^+ \rightarrow \pi^+ \gamma \gamma$  amplitude from different intermediate states. Figure 11 gives the diagrams for some of these processes. These models will be briefly discussed in order of decreasing predicted total branching ratios.

The largest contribution to the amplitude is obtained by using a  $0^+$  meson as an intermediate state [see Fig. 11(a)]. Lapidus<sup>18</sup> uses the assumed  $\sigma$  particle (mass  $\approx 400$  MeV, width  $\approx 100$  MeV) and predicts a branching ratio of  $4 \times 10^{-3}$  with the  $\pi^+$  spectrum peaking for low-energy pions. Oppo and Oneda<sup>19</sup> mention the possibility that an assumed  $\epsilon$  (mass  $\approx 700$  MeV) could enhance the  $K^+ \rightarrow \pi^+ \gamma \gamma$  rate. Unfortunately for these models, there is no evidence that the  $\sigma$  exists, and the  $\epsilon$  resonance that was found has features considerably different from those considered by Oppo and Oneda. For example, the  $\epsilon$  decays exclusively into the  $\pi\pi$  mode.<sup>20</sup>

The axial-vector-dominance model uses a  $1^+$  meson as an intermediate state [Fig. 11(c)]. Intemann has predicted a branching ratio between  $1.4 \times 10^{-4}$  and  $2.1 \times 10^{-4}$  using this model.<sup>21</sup>

The next largest contribution comes from a consideration of the  $K_{\pi 2}$  amplitude with the  $\pi^0$  off the mass shell [see Fig. 11(a),  $\pi^0$  pole model]. Lapidus<sup>18</sup> and Vanyashin,<sup>22</sup> using the usual weak-interaction couplings, conclude that this contribution is negligibly small. Lapidus notes that there is less than a  $10^{-7}$  probability of observing a  $\pi^0$  more than 2 MeV off the mass shell. However, Fujii<sup>17</sup> uses a model in which this amplitude is linear in the

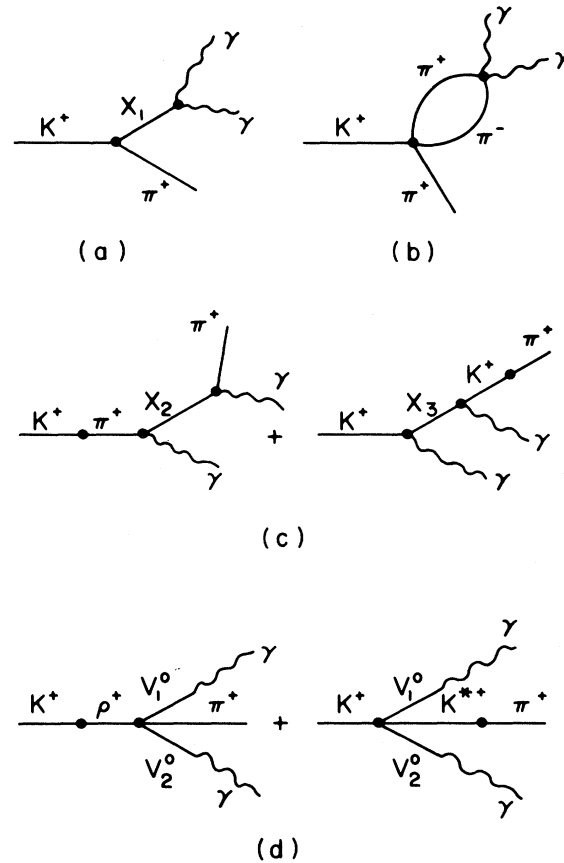


FIG. 11. Diagrams for the direct process  $K^+ \rightarrow \pi^+ \gamma \gamma$ . (a) Single-particle intermediate state:  $0^+$  resonant state ( $X_1 = 0^+$ );  $\pi^0$ -pole model ( $X_1 = \pi^0$ );  $\eta$ -pole model ( $X_1 = \eta^0$ ). (b) Annihilation of virtual  $\pi$ - $\pi$  pair. (c) Axial-vector-dominance model ( $X_2 = A_1^+$  or  $B^+$ ,  $X_3 = K_A^+$ ). Vector-dominance model ( $X_2 = \rho^+$ ,  $X_3 = K^{*+}$ ). (d) Four-particle vertex.

squared momenta of the pions. In this model the amplitude varies with an adjustable parameter  $\epsilon$ , and Fujii estimates  $|\epsilon| \approx 20$  from a consideration of the decays  $K_s^0 \rightarrow \pi^+ \pi^-$  and  $K^+ \rightarrow \pi^+ \pi^0$ . Using this value<sup>23</sup> for  $\epsilon$  and the differential decay rate for  $K^+ \rightarrow \pi^+ \gamma \gamma$  appropriate to this model,<sup>24</sup> one obtains a total branching ratio of  $8 \times 10^{-5}$  for  $K^+ \rightarrow \pi^+ \gamma \gamma$ . In this model the  $\pi^+$  spectrum has a sharp peak in the  $K_{\pi 2}$  region and a large bump for low-energy pions. An unattractive feature of this model is that it is equivalent to using derivative couplings for weak interactions.

Moshe and Singer<sup>25</sup> have considered the four-particle vertices' diagrams shown in Fig. 11(d). With SU(3)-breaking effects, they predict a rate in the range  $0.6 \times 10^{-5} - 2 \times 10^{-5}$ . Their pion spectrum is nearly constant.

At the  $10^{-6}$  level there are two possible contributions to the direct amplitude. Vanyashin<sup>22</sup> con-

siders both virtual  $\pi$ - $\pi$  annihilation<sup>26</sup> and the  $\eta$ -pole model as shown in Figs. 11(b) and 11(a). First he writes a general matrix element for the decay and shows that the pion spectrum is peaked for low-pion energies, while the photon spectrum will peak at high-energy photons. When specifically considering the above two diagrams, he concludes that their contributions are about equal, and that there is no interference between them. He predicts a total branching ratio of  $2 \times 10^{-6}$ . Fildt *et al.*<sup>27</sup> obtain a branching ratio of  $1.5 \times 10^{-6}$  with the kinetic energy of the  $\pi^+$  less than 70 MeV using just the  $\eta$ -pole model. In a variation of the  $\eta$ -pole model, Brown *et al.*<sup>28</sup> consider radiative corrections to  $\eta$ - $\pi$  mixing and obtain a branching ratio of  $3.4 \times 10^{-4}$ .

Finally, down several more orders of magnitude the vector-meson-dominance graphs [Fig. 11(c)] are estimated to be at the  $3 \times 10^{-8}$  to  $4.6 \times 10^{-10}$  level.<sup>17, 21</sup>

### B. Experimental Review

Chen *et al.*<sup>24</sup> did a counter experiment searching for  $K^+ \rightarrow \pi^+ \gamma \gamma$  in which the pion kinetic energy was between 60 and 90 MeV. Assuming the decay proceeds by a  $\sigma$ -meson intermediate state [Fig. 11(a)], they placed an upper limit of  $3.3 \times 10^{-4}$  on the total branching ratio. Thus, their result is inconsistent with the Lapidus model. In the Fujii model, their result is that  $|\epsilon| < 30$ , and hence they do not rule out his prediction. Assuming a phase-space model for the pion spectrum, they quote an upper limit of  $1.1 \times 10^{-4}$  for the total branching level at the 90% confidence level. Klems *et al.*<sup>29</sup> report a total branching-ratio upper limit of  $4.5 \times 10^{-5}$  at the 90% confidence level, assuming a phase-space model. As their counter setup was sensitive to pions above the  $K_{\pi 2}$  region (pion kinetic-energy range 117 MeV–127 MeV), they were unable to check the Fujii model.

### C. Selection of $K^+ \rightarrow \pi^+ \gamma \gamma$ Candidates

The scanners searched for a stopped- $K^+$  decay with two  $\gamma$ 's pointing to the origin. The secondary was required to stop and decay in a  $\pi$ - $\mu$ - $e$  chain, to have no large-angle scatters, and to have a range outside of the  $K_{\pi 2}$  region. Pion identification was provided by the observation of the muon ( $\mu$  pip) in the  $\pi$ - $\mu$ - $e$  decay chain. 1900 events were fitted to the four-constraint  $K^+ \rightarrow \pi^+ \gamma \gamma$  hypothesis, using all measured variables plus the two-constraint hypothesis, ignoring the measured  $\gamma$  energies. Three cuts were applied to all fits. The first cut accepted only those fits with a  $\chi^2$  probability for the  $K^+ \pi^+ \gamma \gamma$  fit greater than 0.01. The second cut discarded any fits in which the fitted pion momentum differed by more than 10.5 MeV from the

measured momentum. Finally, any fits with a fitted pion momentum in the  $K_{\pi 2}$  region from 197 MeV/c to 211 MeV/c were discarded. There were 47 events in which either the 4C fit or the 2C fit, or both, passed the above cuts. Figure 12 shows the  $\chi^2$  distribution for the 4C fit for these events. Also shown is the  $\chi^2$  distribution obtained from fitting  $K_{\pi 2}$  events to the 4C  $K^+ \rightarrow \pi^+ \gamma \gamma$  hypothesis (that is, a one-vertex fit neglecting the  $\pi^0$ ). Except for an overabundance of events in the tail, the  $K_{\pi 2}$   $\chi^2$  distribution is what one would expect for a 4C fit.

The remaining 47 candidates were carefully edited on a scan table by a physicist. The purpose here was to see if the events really satisfied the criteria to be a  $2\gamma\pi$  event. 23 events were discarded for not having a  $\mu$  pip. They were mostly  $K_{\mu 3}$  decays. Two events were discarded because they had a large-angle scatter, and hence they were examples of  $K_{\pi 2}$  decays whose range had been shortened by a strong interaction. Most of the remaining events that were discarded had three  $\gamma$ 's pointing and presumably were  $\tau'$  decays. A total of six events survived editing. Figure 12 also shows the  $\chi^2$ 's for these events. Note that the  $\chi^2$  distribution for these events shows no improvement over that for the 47 events, and also that it does not fit the expected 4C  $\chi^2$  distribution. Thus, some, if not all, of these events are expected to be background.

A background study was made to see what types of background are expected at this level. It was found that one of the six events could be interpreted as an example of  $K^+ \rightarrow \pi^+ \gamma \gamma$  or else as an example of  $K^+ \rightarrow \pi^+ \pi^0 \gamma$ , where one of the  $\pi^0$   $\gamma$ 's had failed to convert. Since the radiative  $K_{\pi 2}$  branching ratio is at the  $10^{-4}$  level, it was important to determine

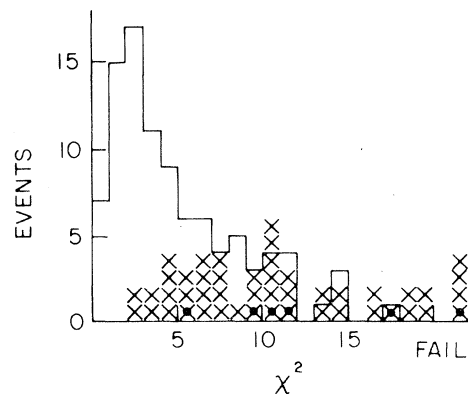


FIG. 12.  $\chi^2$  distribution for four-constraint fit to  $K^+ \rightarrow \pi^+ \gamma \gamma$ . The histogram outlined by a solid line represents 96  $K_{\pi 2}$  events. X represents one of 47  $K^+ \rightarrow \pi^+ \gamma \gamma$  candidates that survive cuts 1–3. ● represents one of six of these 47 candidates that survive editing.

whether it could reasonably be background for  $K^+ \rightarrow \pi^+ \gamma \gamma$  at the  $10^{-5}$  level. A model of radiative  $K_{\pi 2}$  faking  $K^+ \rightarrow \pi^+ \gamma \gamma$  was constructed based on the measurement errors in this experiment, and a consideration of the 21 radiative  $K_{\pi 2}$  events with three converted  $\gamma$ 's found in the radiative  $K_{\pi 2}$  study. The model predicted that an experiment of this type had a 30% chance of having a radiative  $K_{\pi 2}$  event with only two converted  $\gamma$ 's that would pass editing and cuts one through three, and hence be background for  $K^+ \rightarrow \pi^+ \gamma \gamma$ . Estimates were made of the number of events expected from other sources of background, and it was found reasonable to interpret these six events as three  $\tau'$  decays in which only two  $\gamma$ 's converted in the chamber, one  $K_{\mu 3}$  decay in which the muon has a fake  $\mu$  pip, one  $K_{\pi 2}$  decay in flight, and one radiative  $K_{\pi 2}$  decay in which one of the three  $\gamma$ 's failed to convert.

A real  $K^+ \rightarrow \pi^+ \gamma \gamma$  decay is coplanar. That is, the momenta of the pion and the two  $\gamma$ 's are constrained to lie in a plane. No such constraint applies to the background decays, and hence the background only accidentally approximates coplanarity. Thus, in order to separate out the background decays mentioned above from any real signal, one can use a more stringent coplanarity constraint than that provided by the rather loose  $\chi^2$  cut on the over-all fit. To measure how well a given event fits this criteria, define the box product:

$$\text{Box product} = \frac{(\vec{p}_{\pi^+} \times \vec{p}_{\gamma 1}) \cdot \vec{p}_{\gamma 2}}{|\vec{p}_{\pi^+}| |\vec{p}_{\gamma 1}| |\vec{p}_{\gamma 2}|},$$

where all momenta are measured momenta. The range of the box product is  $-1$  to  $+1$ , and a real event will have a box product consistent with zero. Thus, the final cut rejected events with the absolute value of the box product greater than 0.140. Figure 13 shows the box products for the six remaining events along with the box product for a

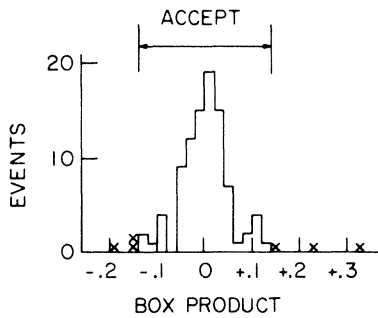


FIG. 13. Coplanarity cut applied to  $K^+ \rightarrow \pi^+ \gamma \gamma$  candidates. The box product is calculated from measured  $\pi^+$  and  $\gamma$  angles. X represents one of six  $K^+ \rightarrow \pi^+ \gamma \gamma$  candidates. The histogram outlined by a solid line represents coplanar  $K_{\pi 2}$  decays.

sample of  $K_{\pi 2}$  decays calculated from the pion and two  $\gamma$  momenta. All six remaining candidates were eliminated by this cut.

#### D. $K^+ \rightarrow \pi^+ \gamma \gamma$ Results

This null result will be discussed in terms of several of the theoretical models. For all models the total detection efficiency is calculated as follows<sup>30</sup>:

$$E_{\text{total}} = N_1 \times N_2 \times N_3 \times N_4 \times N_5 \times N_6,$$

where

$$N_1 = \frac{\int_{T_{\pi^+}} n_1(T_{\pi^+}) \times n_2(T_{\pi^+}) \times n_3(T_{\pi^+}) (d\Gamma/dT_{\pi^+}) dT_{\pi^+}}{\int_{T_{\pi^+}} (d\Gamma/dT_{\pi^+}) dT_{\pi^+}};$$

$n_1$ ,  $n_2$ , and  $n_3$  are the efficiencies considering losses due to strong interactions, leaving secondaries and range cuts as discussed in Secs. II G, II H, and III (see Figs. 3, 5, and 6);  $(d\Gamma/dT_{\pi^+})$  is the differential pion spectrum for the model being considered and the integration is over the pion kinetic energy range being considered.

In actual practice  $N_1$  is found by numerical integration as  $n_1$ ,  $n_2$ , and  $n_3$  are not expressed analytically.

$N_2$  = the chance a pion secondary will be edited by a physicist as having a  $\mu$  pip. It is equal to 0.531 as discussed in Sec. II F;  $N_3$  = the  $\mu$  pip scanning efficiency as discussed in Sec. II F (equal to 0.844, 0.713, or 0.886 depending on the scan);  $N_4$  =  $\gamma$  detection probability for finding two  $\gamma$ 's. As discussed in Sec. II K this is the product of the  $\gamma$  conversion probability and the scanner's  $\gamma$  efficiency. Since the number is dependent on  $\gamma$  energy, it varies slightly depending on the model being considered (0.64 for phase space, 0.656 for Fujii and  $\eta$ -pole models);  $N_5$  = 0.8, the scanners' pion-event detection efficiency as discussed in Sec. II J;  $N_6$  = the efficiencies considering losses due to the cut applied to the candidates. This also includes losses due to failure of event to reconstruct even after three measurements;  $E_{\text{total}}$  is calculated separately for each of the scans and an appropriate average is found. Then with no events the upper limit on the branching ratio is

$$\text{branching ratio} < \frac{2.3}{(\text{average } E_{\text{total}}) \times (\text{total } K^+ \text{ scanned})}$$

at the 90% confidence level.

For  $K^+ \rightarrow \pi^+ \gamma \gamma$ ,  $N_6$  was determined to be 0.93 by applying the four cuts to a sample of  $K_{\pi 2}$  decays. The  $\chi^2$  test was found to be the only cut that discarded any sizable fraction of events.

For the Fujii model, the differential pion spectrum as calculated by Chen *et al.*<sup>24</sup> was used in the

calculation of  $N_1$ .  $N_1$  was found to be close to 84% for  $T_{\pi^+} < 102$  MeV and for all  $|\epsilon| < 50$  except for  $\epsilon$  very near zero. Figure 14 shows the theoretical pion spectrum for the Fujii model, and the dashed line shows the effect of  $N_1$  on the spectrum for  $\epsilon = +11$ . The average  $E_{\text{total}}$  was 19.5%, and the result is

$$\frac{\Gamma(K^+ \rightarrow \pi^+ \gamma \gamma, T_{\pi^+} < 102 \text{ MeV})}{\Gamma(K^+ \rightarrow \text{all})} < 2.2 \times 10^{-5}$$

at the 90% confidence level assuming the Fujii model.

This corresponds to a limit on  $\epsilon$  of  $|\epsilon| < 11$ . Finding a single event in this experiment would have corresponded to  $|\epsilon| \approx 7$ . Thus, this experiment is inconsistent with Fujii's expectation of  $|\epsilon| \approx 20$ .

A constant pion spectrum was assumed in order to calculate the upper limit in the model of Moshe and Singer. The result is

$$\frac{\Gamma(K^+ \rightarrow \pi^+ \gamma \gamma)}{\Gamma(K^+ \rightarrow \text{all})} < 2.9 \times 10^{-5}$$

over the entire spectrum at the 90% confidence level. This upper limit is just above their predicted range.

To compare our results with the  $\eta$ -pole model, the form of the differential pion spectrum as given by Fäldt *et al.*<sup>27</sup> is used:

$$\frac{d\Gamma}{dT_{\pi^+}} \propto \frac{p_{\pi^+} q^4}{(m_{\eta}^2 - q^2)^2},$$

where  $q$  is the invariant mass of the two  $\gamma$ 's. Figure 15(a) shows the pion spectrum obtained. For the branching ratio they obtain

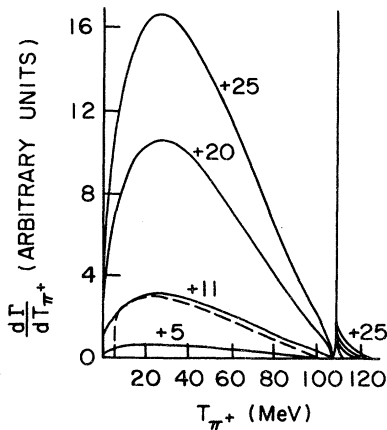


FIG. 14. Theoretical pion spectrum for  $K^+ \rightarrow \pi^+ \gamma \gamma$  using the Fujii model. The different spectra are for the values of  $\epsilon$  given on the figure. The dashed line shows the experimental spectrum for  $\epsilon = 11$ .

$$\frac{\Gamma(K^+ \rightarrow \pi^+ \gamma \gamma, T_{\pi^+} < 70 \text{ MeV})}{\Gamma(K^+ \rightarrow \text{all})} = 1.5 \times 10^{-6}.$$

Our result with  $N_1 = 0.859$  and average  $E_{\text{total}} = 20.3\%$  is

$$\frac{\Gamma(K^+ \rightarrow \pi^+ \gamma \gamma, T_{\pi^+} < 70 \text{ MeV})}{\Gamma(K^+ \rightarrow \text{all})} < 2.1 \times 10^{-5}$$

at the 90% confidence level. Thus, we are an order of magnitude away from testing the  $\eta$ -pole model. However, this result also applies to the modified  $\eta$ -pole model of Brown *et al.*, and clearly their prediction of  $3.4 \times 10^{-4}$  is inconsistent with this experiment.

Finally, Fig. 15(b) shows the pion spectrum obtained from using a phase-space model with

$$\frac{d\Gamma}{dT_{\pi^+}} = \lambda p_{\pi^+},$$

$\lambda = \text{constant}$ .

$N_1$  is 0.552 over the entire spectrum and its effect is shown in Fig. 15(b) as the dashed line. The average  $E_{\text{total}}$  is 12.2% and our result is

$$\frac{\Gamma(K^+ \rightarrow \pi^+ \gamma \gamma)}{\Gamma(K^+ \rightarrow \text{all})} < 3.5 \times 10^{-5}$$

over the entire spectrum at the 90% confidence level. When combined with the result of Klems *et al.*,<sup>29</sup> one obtains a world upper limit of  $2 \times 10^{-5}$ .

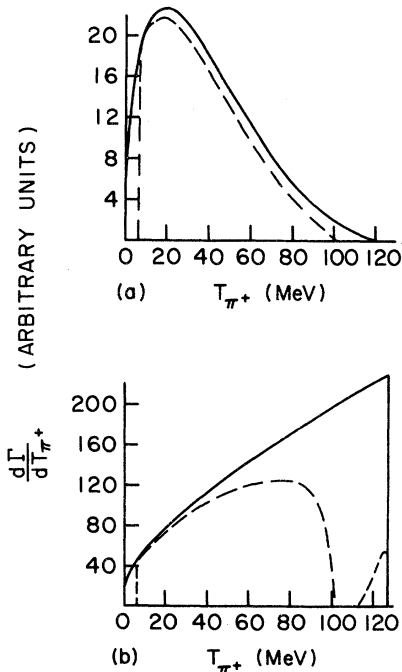


FIG. 15. Theoretical pion spectra for  $K^+ \rightarrow \pi^+ \gamma \gamma$ . The dashed lines show the spectra with experimental efficiencies folded in. (a)  $\eta$ -pole model. (b) Phase space.



The pion spectrum of the axial-vector-dominance model is similar to phase space, and thus our result is inconsistent with this model's prediction of  $(1.4 - 2.1) \times 10^{-4}$ .

In conclusion, the results of this experiment are inconsistent with the predictions made by the Fujii  $\pi^0$ -pole model, the modified  $\eta$ -pole model of Brown *et al.*, and the axial-vector-dominance model of Intemann. The next logical experiment to search for  $K^+ \rightarrow \pi^+ \gamma \gamma$  would be one designed to reach the  $10^{-6}$  level. At this level the  $\eta$ -pole and  $\pi$ - $\pi$  annihilation models as well as the prediction of Moshe and Singer can be tested. A feature of many of the theoretical models for the direct process is the peaking of the pion spectrum at the low-energy end. Thus, a future experiment should search in the region below the  $K_{\pi_2}$  and ideally should include the  $\tau'$  region.

## VI. SEARCH FOR SEMILEPTONIC NEUTRAL CURRENTS: $K^+ \rightarrow \pi^+ \nu \bar{\nu}$

### A. Theoretical and Experimental Review

In the study of weak-interaction physics neutral currents pose an important and as yet unsolved problem. Experimentally, semileptonic interactions involving neutral currents have not been observed, but theoretically, it is difficult to imagine why they do not exist. In first-order weak-interaction theory the decay  $K^+ \rightarrow \pi^+ \nu \bar{\nu}$  would be due to the coupling of a neutral hadronic current and a neutral leptonic current. Experimental studies of interactions involving  $e^+ e^-$  or  $\mu^+ \mu^-$  pairs have failed to observe neutral currents. Prior to any systematic experimental studies of interactions involving neutrino pairs, Weiner<sup>31</sup> and Oakes<sup>32</sup> suggested models in which only neutral leptonic currents involving neutrinos exist. Oakes<sup>33</sup> predicted a branching ratio for  $K^+ \rightarrow \pi^+ \nu \bar{\nu}$  of  $1.8 \times 10^{-5}$ . Thus, despite the experimental difficulties, it was important to search for an interaction involving neutrino pairs, such as  $K^+ \rightarrow \pi^+ \nu \bar{\nu}$ , before the possibility of neutral currents appearing in first order could be ruled out.

Experimentally, Cline<sup>34</sup> obtained an upper limit of  $7.6 \times 10^{-4}$  for this decay with pion kinetic energy in the range 55–98 MeV. Preliminary results on the present experiment<sup>1</sup> were an upper limit of  $1.0 \times 10^{-4}$  over the entire spectrum. In a counter experiment, Klems *et al.*<sup>29</sup> definitely eliminated the chance that neutral currents would be observed as a first-order phenomena. They established an upper limit of less than  $7.5 \times 10^{-7}$  over the entire vector spectrum by looking in the regions  $60 < T_{\pi^+} < 100$  MeV,  $117 < T_{\pi^+} < 127$  MeV.

Renormalizable theories<sup>35</sup> of weak interactions

and theories of  $CP$  violation<sup>36, 37</sup> predict that  $K^+ \rightarrow \pi^+ \nu \bar{\nu}$  will appear at about the  $10^{-7}$  level. Aside from the predictions of these rather complicated theories, the decay is expected to occur as a second-order weak interaction. In order to avoid infinities, a cutoff must be made when doing the second-order calculation. Using a cutoff of 300 BeV, Segrè<sup>38</sup> obtains a branching ratio of  $2 \times 10^{-5}$ . Willey<sup>39</sup> uses the limit on  $K_L^0 \rightarrow \mu^+ \mu^-$  to obtain a limit of  $4 \times 10^{-11}$  for  $K^+ \rightarrow \pi^+ \nu \bar{\nu}$ . Singh and Wolfenstein<sup>37</sup> predict a second-order branching ratio of  $6 \times 10^{-14}$ . Theoretically,  $K^+ \rightarrow \pi^+ \nu \bar{\nu}$  offers a good chance to study second-order effects as second order is not competing with first order plus electromagnetic effects as in  $K^+ \rightarrow \pi^+ e^+ e^-$ . If branching ratios at this level could be studied, one might observe nonlocal effects in weak interactions.<sup>37</sup>

### B. Experimental Search

The decay  $K^+ \rightarrow \pi^+ \nu \bar{\nu}$  is underconstrained as only the incoming  $K^+$  and the outgoing  $\pi^+$  can be observed. Kinematically one can determine the momentum of the pion ( $p_{\pi^+}$ ) from its range and the angle between the incident  $K^+$  direction and the outgoing  $\pi^+$  direction ( $\theta_{K\pi}$ ). Also, an upper limit on the  $K^+$  momentum can be set. Stopping- $K^+$  decays are separated from in-flight decays by observing the ionization of the last few centimeters of  $K^+$  flight. Studies of in-flight  $K_{\pi_2}$  decays indicated that  $K^+$  decays in flight with  $K^+$  momentum greater than 200 MeV/c have noticeably lighter ionization for the  $K^+$  track. However, below that momentum the  $K^+$  ionization of an in-flight decay is indistinguishable on the scan table from the  $K^+$  ionization of a stopped decay. Thus, an upper limit of 200 MeV/c can be set for the  $K^+$  momentum. The search for this decay relies on the fact that for  $K^+$  decays with an identified pion secondary, one can use the above information to eliminate kinematically any events that might be background. Fortunately, one can make cuts that eliminate all background down to the  $10^{-5}$  level and still leave "search areas" in which only  $K^+ \rightarrow \pi^+ \nu \bar{\nu}$  decays are expected. The details are as follows.

Positive pion identification is provided by observation of the pion's decay into a muon, which then decays into an electron. In order to obtain an accurate measurement of the pion's momentum by range, the scanners were instructed to accept only pion secondaries without kinks (strong interactions). The background level due to the ordinary  $K^+$  decays with one or more  $\pi^0$ 's in the final state ( $K_{\pi_2}$ ,  $\tau'$ ,  $K_{\mu_3}$ ) is suppressed (approximately  $10^{-2}$ ) by accepting only decays that have no  $\gamma$ 's pointing to the decay origin. Also, ordinary two-body decays with a fixed secondary range ( $K_{\pi_2}$  and  $K_{\mu_2}$ )

were suppressed at the scan table by the use of a projected range template. The scanners found 419  $0\gamma\pi$  events.

These events were measured and any remaining stopped- $K_{\pi 2}$  or  $K_{\mu 2}$  decays were eliminated by discarding pion secondaries with a momentum by range between 196.2 and 212.3 MeV/c, or greater than 238.7 MeV/c. After this cut there were 143 remaining events, and these were edited by a physicist to make certain that they fitted the scanning criteria. Events were discarded for having a  $\gamma$  pointing, for having a kink, for not having an acceptable  $\mu$  pip and so on. Only 11 events remained and their  $p_{\pi^+}$  and  $\theta_{K\pi}$  are plotted on Fig. 16. The final cut was to eliminate all events with  $p_{\pi^+}$  and  $\theta_{K\pi}$  in the kinematic regions allowed to the following in-flight decays:

$$K^+_{\text{in flight}} \rightarrow \pi^+ \pi^0 (K_{\pi 2}),$$

$$K^+_{\text{in flight}} \rightarrow \mu^+ \nu (K_{\mu 2}),$$

with  $p_{K^+} < 200$  MeV/c at time of decay. In the case of in-flight  $K_{\pi 2}$  decays, this cut basically means one eliminates forward  $K^+$  decays with secondary ranges greater than the stopped  $K_{\pi 2}$  range and backward decays with short ranges. The cut on  $K_{\mu 2}$  decays is required since a small fraction of muon secondaries can have a fake  $\mu$  pip. Thus, a backward in-flight  $K_{\mu 2}$  decay with a fake  $\mu$  pip can appear as background to  $K^+ \rightarrow \pi^+ \nu \bar{\nu}$ . The kinematic regions eliminated are indicated in Fig. 16 by hatched areas. Note 10 of the candidates are elim-

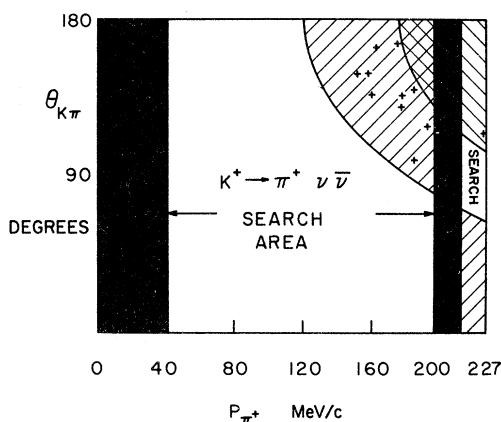


FIG. 16. Scatter plot of  $\pi^+$  momentum determined by range and the angle between the outgoing  $\pi^+$  and the incident  $K^+$ . Events in the shaded bands have been eliminated. Below 41 MeV/c the pion cannot be identified and pions from stopped  $K_{\pi 2}$  decays are expected to fall in the band 196 to 212 MeV/c. The hatched regions are accessible to in-flight  $K_{\pi 2}$  decays (/ /) and in-flight  $K_{\mu 2}$  decays (\ \) ( $K^+$  momentum less than 200 MeV/c). The two "search areas" are expected to be free of background.

inated by the  $K_{\pi 2}$  cut, and one is discarded by the  $K_{\mu 2}$  cut. No  $K^+ \rightarrow \pi^+ \nu \bar{\nu}$  candidates remained.

### C. Upper Limit on $K^+ \rightarrow \pi^+ \nu \bar{\nu}$ Branching Ratio

One can make crude estimates of the best results obtainable in a bubble chamber experiment of this type.  $K_{\pi 2}$  and  $K_{\mu 2}$  background is eliminated as described above. Another possible source of background is a radiative  $K_{\mu 2}$  decay in which the  $\gamma$  escapes detection and the muon has a fake  $\mu$  pip. Calculations indicated that this background is an order of magnitude below the level of this experiment. Ordinary  $\tau'$  decays in which all four  $\gamma$ 's leave the chamber before conversion have a very low rate due to the large size of the chamber as compared with the short radiation length. Also, the above two sources of background can be eliminated by kinematic cuts if necessary. However, the ordinary  $K_{\mu 3}$  decay with a fake  $\mu$  pip and two missing  $\gamma$ 's is background at about the  $10^{-5}$  level. Since the  $K_{\mu 3}$  muon spectrum completely overlaps the  $K^+ \rightarrow \pi^+ \nu \bar{\nu}$  pion spectrum, this background cannot be eliminated kinematically. Thus, this method can only be pushed to about  $10^{-5}$  level.

The upper limit on the  $K^+ \rightarrow \pi^+ \nu \bar{\nu}$  branching ratio actually reached in this experiment was determined by calculating the detection efficiency for finding real events. Considered in the calculation was the probability of observing a  $\mu$  pip, the efficiency for finding the secondaries, losses due to strong interactions, losses due to secondaries leaving the chamber, losses due to the various range cuts, and losses due to the cuts on in-flight decays. Included in the range losses was a very small loss due to the fact that short pions (<2 mm) cannot be identified. The calculation was done separately for each of the following assumed first-order pion spectra<sup>29</sup>:

Assumed first-order interaction	$d\Gamma/dT_{\pi^+}$
vector	$p_{\pi^+}^3$
tensor	$p_{\pi^+}^3(T_M - T_{\pi^+})$
scalar	$p_{\pi^+}(T_M - T_{\pi^+})$

where:  $p_{\pi^+}$  = pion momentum,  
 $T_{\pi^+}$  = pion kinetic energy, and  
 $T_M$  = maximum kinetic energy allowable for  $K^+ \rightarrow \pi^+ \nu \bar{\nu}$  (127 MeV). Figure 17 shows these spectra. The over-all efficiencies are 11.0, 20.1, and 27.3% for vector, tensor, and scalar interactions, respectively.

A total of 367 500 stopped  $K^+$  were scanned. Thus, the upper limits determined by this experiment are

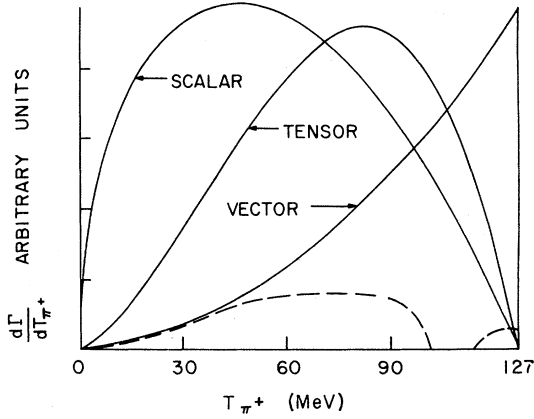


FIG. 17. Theoretical pion spectrum for  $K^+ \rightarrow \pi^+ \nu \bar{\nu}$  assuming vector, tensor, or scalar first-order interaction. The dashed line shows the expected experimental spectrum for the vector interaction.

$$\frac{\Gamma(K^+ \rightarrow \pi^+ \nu \bar{\nu})}{\Gamma(K^+ \rightarrow \text{all})} < 5.7 \times 10^{-5} \quad (\text{vector}),$$

$$< 3.1 \times 10^{-5} \quad (\text{tensor}),$$

$$< 2.3 \times 10^{-5} \quad (\text{scalar}).$$

All limits are at the 90% confidence level.

The vector result is to be compared with our preliminary results of  $< 1.0 \times 10^{-4}$ . In conclusion, no evidence for neutral currents involving neutrino pairs was found. This experiment is the only one to study the pion spectrum below 60 MeV kinetic energy, however, the results of the counter experiments<sup>29</sup> put more stringent limits on this decay mode.

## VII. OBSERVATION OF $K_{e4}$ ,

### A. Theoretical Review

Consider the decays:

$$K^+ \rightarrow \pi^+ \pi^- e^+ \nu \quad (K_{e4})(A),$$

$$K^+ \rightarrow \pi^0 \pi^0 e^+ \nu \quad (K_{e4})(B),$$

$$K^0 \rightarrow \pi^0 \pi^- e^+ \nu \quad (C).$$

The matrix element for these decays is given by<sup>40, 41</sup>

$$(2\pi)^4 \delta^{(4)}(p_k - p_+ - p_- - p_e - p_\nu) (G/\sqrt{2})$$

$$\times [\bar{\nu} \gamma_\lambda (1 + \gamma_5) e] \langle \pi\pi | J_\lambda^V + J_\lambda^A | K \rangle.$$

$J_\lambda^V$  is the hadron vector-current and  $J_\lambda^A$  is the axial-vector current, which are given by invariance considerations as

$$\langle \pi\pi | J_\lambda^A | K \rangle = \frac{f_1}{M_K} (p_+ + p_-)_\lambda + \frac{f_2}{M_K} (p_+ - p_-)_\lambda$$

$$+ \frac{f_3}{M_K} (p_e + p_\nu)_\lambda,$$

$$\langle \pi\pi | J_\lambda^V | K \rangle = \frac{f_4}{M_K^3} \epsilon_{\lambda\alpha\beta\gamma} (p_e + p_\nu)_\alpha$$

$$\times (p_+ + p_-)_\beta (p_+ - p_-)_\gamma,$$

where  $f_1$ ,  $f_2$ ,  $f_3$ , and  $f_4$  are dimensionless form factors. In this paper we shall consider  $K_{e4}$  decays (decay B). In this case  $f_2$  and  $f_4$  are zero due to Bose statistics and the  $\Delta I = \frac{1}{2}$  rule,<sup>41</sup> and the following relationships are obtained<sup>42</sup>:

$$\Gamma(B) = \frac{1}{2} \Gamma(A) - \frac{1}{4} \Gamma(C) \quad (1)$$

and<sup>41</sup>

$$\Gamma(B) = a |f_1|^2 + c |f_3|^2 + f |f_1| |f_3|;$$

$$a = 1.59 \times 10^3 \text{ sec}^{-1},$$

$$c = 2.50 \times 10^{-3} \text{ sec}^{-1},$$

$$f = 2.93 \times 10^{-2} \text{ sec}^{-1}. \quad (2)$$

Several theoretical models have been used to calculate the  $K_{e4}$  form factors.<sup>43</sup> In general, the theories agree well enough among themselves so that a low statistics  $K_{e4}$  experiment would not be able to differentiate among them. However, all of the models predict that  $f_1$  and  $f_3$  for the  $K_{e4}$  decay are of order unity. Thus, from Eq. (2) above, the major contribution to the rate is due to  $f_1$ , and so an experimental rate determination can be used to calculate  $f_1$ . Another result of the  $\Delta I = \frac{1}{2}$  rule is that  $f_1$  for decay A is equal to  $f_1$  for decay B, and hence this can be experimentally checked. Another similarity of the various models is that  $\Gamma(C)$  is small and thus  $\Gamma(B)/\Gamma(A)$  only varies from 0.39 to 0.47 [consider Eq. (1)]. In conclusion, a low-statistics  $K_{e4}$  experiment can be used to determine the rate and  $f_1$ . Any deviation from the expected results would indicate a deviation from the  $\Delta I = \frac{1}{2}$  rule. Previously, the only experimental result on  $K_{e4}$  was given by Romano *et al.*<sup>44</sup>:

$$\frac{\Gamma(K^+ \rightarrow \pi^0 \pi^0 e^+ \nu)}{\Gamma(K^+ \rightarrow \text{all})} < 1.8 \times 10^{-4} \quad (90\% \text{ confidence level}).$$

### B. Selection of Events and Background Discussion

The decay mode  $K^+ \rightarrow \pi^0 \pi^0 e^+ \nu$  was searched for by having scanners look for electron secondaries with four converted  $\gamma$ 's pointing to the decay origin.  $\gamma$ 's that could reasonably be interpreted as bremsstrahlung were discarded by scanners. 674 200 stopped- $K^+$  in the fiducial volume were scanned, and 148 candidates were found and measured. These events were fitted to the three-ver-

tex three-constraint fit for  $K_{e4}$ , and only events with a  $\chi^2$  probability of greater than 0.001 were accepted (cut number 1).

A cut was also applied to the data to eliminate events where one  $\gamma$  could have come from bremsstrahlung of the electron secondary. This cut amounted to eliminating any event where any of the four  $\gamma$ 's had a measured angle relative to the electron direction of less than  $15^\circ$  (cut number 2).

48 events survived these two cuts and were edited by a physicist to see if the events were really four  $\gamma$  electron events. In this editing the secondary was checked very carefully to make certain it was an electron. Only secondaries in which there was no possible confusion among electron, pion, or muon secondaries were kept. Nine events were left after editing. The discarded events were made up of four  $\gamma$  pion events and electron events in which the scanner had included bremsstrahlung or a  $\gamma$  from another alternate origin as one of the four  $\gamma$ 's. Seven of the nine remaining events have a measured electron momentum less than 60 MeV/c. These events could be examples of collinear  $\tau'$  decays. This is the ordinary decay  $K^+ \rightarrow \pi^+ \pi^0 \pi^0$  in which the  $\pi^+$  carries off only a small amount of momentum. Then, if the  $\pi^+$  and  $\mu^+$  from the  $\pi$ - $\mu$ - $e$  decay chain are not observed, one has an event that appears to have an electron secondary. However, the maximum electron momentum from a  $\pi$ - $\mu$ - $e$  chain is 53 MeV/c. The events with small electron momentum were fitted to the three-vertex three-constraint  $\tau'$  hypothesis, assuming no knowledge of the  $\pi^+$  secondary. Most of these events had a low  $\chi^2$  fit to this collinear  $\tau'$  hypothesis, with a reconstructed  $\pi^+$  of momentum less than 40 MeV/c. Thus, these events were most likely examples of collinear  $\tau'$  decays that faked  $K_{e4}$ . There was one event with a measured electron momentum of 63 MeV/c, and this is just above the  $\tau'$  region. This event was measured four times and each time the collinear  $\tau'$  fit reconstructed a  $\pi^+$  with a momentum of  $94 \pm 8$  MeV/c. A pion with this momentum has a range of 3.5 cm and would definitely be seen on the scanning table, and hence, the collinear  $\tau'$  background is ruled out for this event. Thus, collinear  $\tau'$  events were eliminated by discarding any events with measured electron momentum less than 60 MeV/c (cut number 3). Two candidates are left after this cut.

A  $\tau'$  decay can also be background if it has an energetic  $\pi^+$  and if the entire  $\pi^+ - \mu^+ - e^+$  decay chain fakes the appearance of an electron. Hopefully all of this background was eliminated at the editing stage, but to check for it, the two remaining candidates, along with the events satisfying cuts one through three but discarded earlier because they had a secondary that could be inter-

preted either as an electron or as a pion on the scan table, were all remeasured several times, assuming the secondary to be a pion. These events were fitted to the three-vertex six-constraint  $\tau'$  hypothesis. In general, one would not expect a real  $K_{e4}$  decay to fit  $\tau'$  as  $K_{e4}$  is a four-body decay, while  $\tau'$  is a coplanar three-body decay. The results of this  $\tau'$  fit were that both remaining  $K_{e4}$  candidates failed to reconstruct as a  $\tau'$ , while all the events with ambiguous secondaries had reasonable  $\tau'$  fits. Thus, the necessity of accepting only good electron secondaries is established.

$\tau'$  and  $K_{e4}$  decays are the only expected  $K^+$  decays with four converted  $\gamma$ 's, and  $\tau'$  background has been eliminated as stated above. Thus, any other background must involve an accidental  $\gamma$  or a bremsstrahlung  $\gamma$ . The two remaining candidates were carefully edited, and it was found that all  $\gamma$ 's point well and have no alternate origins anywhere in the chamber. Furthermore, for both events all the  $\gamma$ 's convert within 15 cm of the decay origin. This reduces the likelihood that any of the  $\gamma$ 's are accidental as in general the farther a  $\gamma$  is from an origin, the harder it is to tell that it only points to that origin. Bremsstrahlung has been eliminated by editing and by cut 2, and it is noted that for the two candidates all  $\theta_{e\gamma}$  are greater than  $30^\circ$  and all  $\theta_{\gamma\gamma}$  (angles between any pair of two  $\gamma$ 's) are greater than  $50^\circ$ . Any other types of background, such as that caused by various in-flight decays, or that caused by  $K^0$  decays, are extremely unlikely and can be ruled out.

Thus, all background has been ruled out and two  $K_{e4}$  events remain. For one of the events, only one possible combination of  $\gamma$ 's making  $\pi^0$ 's had a  $K_{e4}$  fit, while the other event had two combinations. In the ambiguous case, information on the opening angles for the  $\pi^0$  decays did not favor one combination over the other; however, the  $\gamma$  energies as estimated on the scan table matched up best with the fitted energies for the lower  $\chi^2$  fit. Thus, the combination with the lowest  $\chi^2$  was chosen. The fitted variables for the two  $K_{e4}$  events are given in Table I, and Fig. 18 shows one of the events.

### C. $K_{e4}$ , Branching Ratio and Discussion of Results

The  $K_{e4}$  branching ratio as compared with  $K_{e3}$  was calculated. The 4  $\gamma$  detection efficiency as discussed in Sec. II K was used. Also considered was a 5% loss due to cuts 1 and 2, a 6% loss due to the editing criteria for good electrons (see Sec. II E), and a  $40 \pm 5\%$  loss due to cut 3. The loss due to discarding low-energy electrons was calculated from the electron spectrum obtained in a

TABLE I. Fitted variables for two  $K_{e4}$  decays.

Event number	$\chi^2$ for $K_{e4}$ fit	Particle	Azimuth (deg)	Dip (deg)	Momentum (MeV/c)
1	1.3	$e^+$	$184 \pm 3$	$-52 \pm 3$	$137 \pm 13$
		$\pi^0$	$40 \pm 25$	$29 \pm 23$	$54 \pm 21$
		$\pi^0$	$55 \pm 9$	$72 \pm 17$	$77 \pm 6$
		$\nu$	$309 \pm 25$	$9 \pm 21$	$57 \pm 20$
2	5.3	$e^+$	$283 \pm 5$	$26 \pm 8$	$61 \pm 15$
		$\pi^0$	$255 \pm 8$	$-41 \pm 9$	$74 \pm 13$
		$\pi^0$	$116 \pm 1$	$-2 \pm 3$	$149 \pm 14$
		$\nu$	$339 \pm 13$	$21 \pm 18$	$78 \pm 13$

$K_{e4}$  experiment.<sup>45</sup> The total detection efficiency was 23% and 22 952 valid  $K_{e3}$  were found (see Sec. II E), giving a rate for the two  $K_{e4}$  events of

$$\frac{\Gamma(K^+ \rightarrow \pi^0 \pi^0 e^+ \nu)}{\Gamma(K^+ \rightarrow e^+ \pi^0 \nu)} = 3.8 \times 10^{-4}.$$

This implies a branching ratio of<sup>46</sup>

$$\frac{\Gamma(K^+ \rightarrow \pi^0 \pi^0 e^+ \nu)}{\Gamma(K^+ \rightarrow \text{all})} = (1.8^{+2.4}_{-0.6}) \times 10^{-5}.$$

The errors were calculated using the Poisson distribution.

Using Eq. (2) above and assuming only  $f_1$  contributes, one obtains

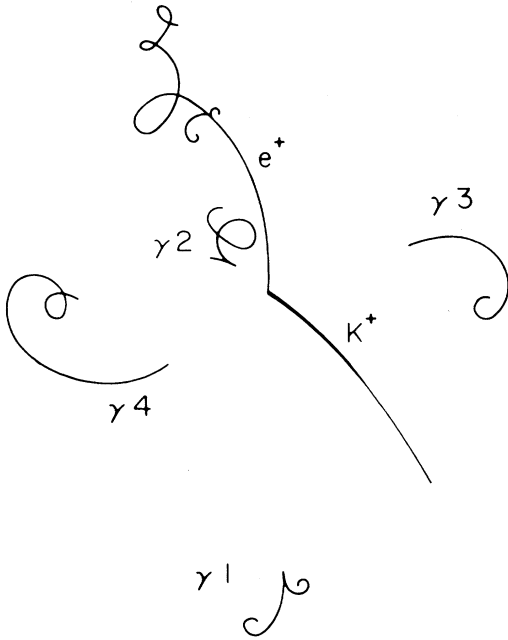


FIG. 18. Sketch of  $K_{e4}$  event number 1.  $\gamma_1$  and  $\gamma_2$  are from the decay of one  $\pi^0$ , and  $\gamma_3$  and  $\gamma_4$  from the other  $\pi^0$ . Note the  $\delta$  rays or bremsstrahlung attached to the electron secondary.

$$|f_1| = 0.97^{+0.50}_{-0.19}.$$

These results are in good agreement with the  $\Delta I = \frac{1}{2}$  rule predictions. The value for the magnitude of  $f_1$  agrees with the value of  $1.19 \pm 0.13$  obtained by Berends *et al.*<sup>47</sup> from an analysis of  $K_{e4}$  data. The experimental  $K_{e4}$  branching ratio is reported<sup>48</sup> as  $(3.3 \pm 0.3) \times 10^{-5}$  and in a recent experiment<sup>49</sup> as  $(4.11 \pm 0.38) \times 10^{-5}$ . Hence, the  $K_{e4}$  branching ratio is compatible with the  $\Delta I = \frac{1}{2}$  prediction given by Eq. (1) above, if one assumes a small rate for  $K^0 \rightarrow \pi^0 \pi^- e^+ \nu$ .

## VIII. EXPERIMENTAL STUDY OF $K^+ \rightarrow e^+ \pi^0 \nu \gamma$

### A. Theoretical and Experimental Review

Theoretically, the decay  $K^+ \rightarrow e^+ \pi^0 \nu \gamma$  has been discussed by Fischbach and Smith.<sup>14</sup> This decay is expected to be dominated by the internal bremsstrahlung contribution, and the interesting structure-dependent terms are expected to contribute less than 1% to the branching ratio. Doncel<sup>50</sup> has pointed out one of the experimental difficulties in detecting radiative  $K_{e3}$ . An experiment must be able to separate internal bremsstrahlung events from external bremsstrahlung off the secondary electron. Doncel suggests a cut on the angle between the  $\gamma$ 's direction and the direction of the secondary electron ( $\theta_{e\gamma}$ ). Thus, he calculates the theoretical branching ratio (using essentially the model described by Fischbach and Smith) as a function of  $\theta_{e\gamma}$  and  $E_\gamma$  ( $E_\gamma$  is the cutoff on low-energy  $\gamma$ 's). The first experimental result was reported by Romano *et al.*<sup>44</sup> In a bubble chamber filled with freon they observed 13 events,<sup>51</sup> and they give the experimental branching ratio for several values of the  $E_\gamma$  cutoff. The value that can be compared with the result of this experiment is

$$\frac{\Gamma(K^+ \rightarrow e^+ \pi^0 \nu \gamma)}{\Gamma(K^+ \rightarrow e^+ \pi^0 \nu)} = (0.53 \pm 0.22) \times 10^{-2}$$

for  $E_\gamma > 30$  MeV and  $0.6 < \cos \theta_{e\gamma} < 0.9$ . Their results as well as the results of this experiment are consistent with the theoretical predictions.

### B. Selection of Events

The scanners searched for stopped- $K^+$  decays with an electron secondary and three associated  $\gamma$ 's. The scanning was done at the same time as the scan for  $K_{e4}$  events. A total of 666 candidates were measured, and then had several cuts applied to them. A  $\chi^2$  cut at the 0.001 probability level was made on the two-constraint radiative  $K_{e3}$  fit. Due to the low scanning efficiency for low-energy  $\gamma$ 's, all events with any  $\gamma$  having a measured energy less than 30 MeV were discarded. Cuts were made to eliminate background due to bremsstrah-

lung  $\gamma$ 's. These cuts are necessary because the common  $K_{e3}$  decay can appear to be a 3  $\gamma$  event due to bremsstrahlung either off the electron secondary or else from the converted electron pairs. Since bremsstrahlung is peaked sharply forward, it can be eliminated by applying a cut to  $\theta_{e\gamma}$  and  $\theta_{\gamma\gamma}$  (the angle between any pair of  $\gamma$ 's). To determine the cutoff on  $\theta_{e\gamma}$ , a sample of electron events with  $\gamma$ 's that could be considered as either pointing directly to the  $K^+$  decay origin or as bremsstrahlung from the first centimeter of electron track was measured. A cutoff for events with a  $\cos\theta_{e\gamma} > 0.9$  was chosen since it eliminated this bremsstrahlung and also allowed direct comparison with the results of Romano *et al.* The cutoff on  $\theta_{\gamma\gamma}$  can be more stringent and all events with any  $\theta_{\gamma\gamma} < 10^\circ$  were discarded. Another source of background is a  $\tau'$  decay with a short undetectable  $\pi^+$ . The electron from the  $\pi-\mu-e$  decay chain can cause this to be scanned as an electron event. Since the kinematic upper limit for these electrons is 53 MeV, this background is eliminated by discarding all events with measured electron energy less than 60 MeV.

The remaining events were carefully edited by a physicist. Background from  $K_{e3}$  decays with an accidental  $\gamma$  was eliminated by checking carefully for alternate origins in a bubble chamber. Also, the secondary electron was checked carefully to make certain it was an electron. In this way pions from  $\tau'$  decays that were incorrectly scanned as electrons were eliminated. It was found necessary to make a further cut to eliminate bremsstrahlung from the electron secondary. The electron can have bremsstrahlung at any point along its path as it spirals in the magnetic field. Bremsstrahlung from the first part of the track is eliminated by the cut on  $\theta_{e\gamma}$ . However, consider the case of bremsstrahlung from the secondary after the secondary's direction has changed significantly from its original direction. If the bremsstrahlung  $\gamma$  converts far enough away from the secondary then it may appear to point equally well as a direct  $\gamma$  from the origin or as bremsstrahlung off the secondary. Thus, events satisfying the following two criteria were discarded: First, the measured angles of the event must be consistent with a  $\gamma$  being tangent to the secondary at some point along the secondary's spiraling path. Second, on the scan table the  $\gamma$  must point both as bremsstrahlung and as a direct  $\gamma$  from the origin. A test for the necessity of this cut can be made in the following manner. First, select all candidates without using the cut. Next, calculate the number of events that would be discarded by applying this cut. Finally, imagine the path the secondary electron would have taken had the magnetic field

been reversed, and again look at the sample of events and see how many events would have been discarded by an application of this cut. The direction of external bremsstrahlung  $\gamma$ 's of course depends on the direction of the magnetic field, while the direction of  $\gamma$ 's coming from the decay origin does not. Thus, the fact that an excess of  $\gamma$ 's was found tangent to the real path of the secondary as compared with the imaginary path means that this cut is needed to eliminate external bremsstrahlung. This method can also be used to estimate the number of real events discarded by the cut.

After editing, 17 events remained. The only remaining source of background is  $K_{e4}$  decays in which only three of the four  $\gamma$ 's convert. From a consideration of the number of 4  $\gamma$   $K_{e4}$  events found in this experiment (two) plus the chance that a  $K_{e4}$  event would survive the radiative  $K_{e3}$  cuts, it was determined that there are  $1 \pm 1$  events due to  $K_{e4}$  background in the 17 events. However, no cut could be made to eliminate this background.

As in the radiative  $K_{\pi 2}$  experiment, an attempt was made to select the extra (the radiative or non- $\pi^0$ )  $\gamma$  in these 17 events by considering the  $\chi^2$ 's for the fits. However, it was found that the events were not constrained enough to allow an unambiguous choice. Figure 19 shows the spectrum for  $\cos\theta_{e\gamma}$  considering all the  $\gamma$ 's. It is the spectrum one would expect for radiative  $K_{e3}$  events.<sup>44</sup> In particular, note the clustering in the forward direction due to the internal bremsstrahlung  $\gamma$ 's. The shaded portion of Fig. 19 shows the spectrum obtained by selecting the single  $\gamma$  with the largest  $\cos\theta_{e\gamma}$  from each event. Although the separation from the rest of the  $\gamma$ 's is not entirely clean, the typical internal bremsstrahlung shape of the

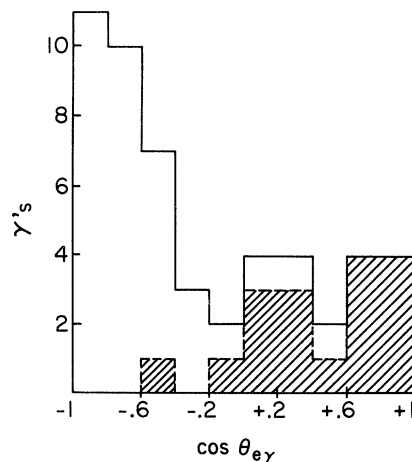


FIG. 19.  $\cos\theta_{e\gamma}$  for the three  $\gamma$ 's in 17 radiative  $K_{e3}$  events. Shading indicates the spectrum for the single  $\gamma$  in each event with the largest  $\cos\theta_{e\gamma}$ .

shaded spectrum suggests that these  $\gamma$ 's are the extra  $\gamma$ 's.

### C. Radiative $K_{e3}$ Branching Ratio

16 events (17 minus one background) were used to calculate a branching ratio relative to  $K_{e3}$  decays. The  $\gamma$  spectrum from Doncel's paper with a 30-MeV cutoff was used in calculating the extra  $\gamma$  conversion probability. The loss due to the cutoff on electron energy was calculated to be 12% from a consideration of the  $K_{e3}$  electron spectrum along with a correction for the difference in spectra between  $K_{e3}$  and radiative  $K_{e3}$ .<sup>44</sup> Editing losses, along with losses due to the  $\chi^2$  cut and the  $\theta_{\gamma\gamma}$  cut were 9%. Thus, the experimental branching ratio is

$$\frac{\Gamma(K^+ \rightarrow e^+ \pi^0 \nu \gamma)}{\Gamma(K^+ \rightarrow e^+ \pi^0 \nu)} = (0.48 \pm 0.20) \times 10^{-2}$$

for  $E_\gamma > 30$  MeV and  $\cos \theta_\gamma < 0.9$ . In order to compare directly with the result of Romano *et al.*, the branching ratio was also recalculated using their

$\cos \theta_\gamma$  spread.  $K_{e4}$  background in this region was calculated to be 0.75 event from a consideration of the 4  $\gamma$   $K_{e4}$  sample:

$$\frac{\Gamma(K^+ \rightarrow e^+ \pi^0 \nu \gamma)}{\Gamma(K^+ \rightarrow e^+ \pi^0 \nu)} = (0.22_{-0.10}^{+0.15}) \times 10^{-2}$$

for  $E_\gamma > 30$  MeV and  $0.6 < \cos \theta_\gamma < 0.9$ . Theoretically, these two rates are  $0.53 \times 10^{-2}$  and  $0.29 \times 10^{-2}$ , respectively.<sup>50</sup> Thus, the model of Fischbach and Smith agrees with the data. However, as their model is dominated by the internal bremsstrahlung contribution, this experiment is not sensitive enough to check the small structure-dependent terms in their model.

### ACKNOWLEDGMENTS

We wish to thank R. Klem, D. Nordby, and V. Sevcik for their cooperation in the running of this experiment at Argonne National Laboratory. One of us (D. L.) wishes to thank Professor Ugo Camerini and Professor W. F. Fry for many helpful discussions.

\*Research supported in part by the U. S. Atomic Energy Commission under Contract No. AT(11-1)-881-343.

†This work is the subject of a thesis submitted by D. Ljung in partial fulfillment of the requirements of the Doctor of Philosophy degree at the University of Wisconsin. Present address: National Accelerator Laboratory, Batavia, Illinois 60510.

<sup>1</sup>U. Camerini, D. Ljung, M. Sheaff, and D. Cline, *Phys. Rev. Lett.* **23**, 326 (1969).

<sup>2</sup>D. Ljung, *Phys. Rev. Lett.* **28**, 523 (1972).

<sup>3</sup>D. Cline and D. Ljung, *Phys. Rev. Lett.* **28**, 1287 (1972).

<sup>4</sup>L. Behr and P. Mittner, *Nucl. Instrum. Methods* **20**, 446 (1963).

<sup>5</sup>See a January 1969 update to "The Complete Shape Manual," by C. T. Murphy (unpublished).

<sup>6</sup>D. Cline, *Phys. Rev. Lett.* **16**, 367 (1966).

<sup>7</sup>G. Costa and P. K. Kabir, *Phys. Rev. Lett.* **18**, 429 (1967).

<sup>8</sup>N. Christ, *Phys. Rev.* **159**, 1292 (1967).

<sup>9</sup>J. D. Good, *Phys. Rev.* **113**, 352 (1959).

<sup>10</sup>B. Wolff, thesis, University of Paris, 1967 (unpublished). See also M. Mezza, thesis, University of Paris (unpublished), and D. Gamba and A. Werbrouck, Torino report (unpublished) (as footnoted in Wolff's thesis).

<sup>11</sup>N. Cabibbo and R. Gatto, *Phys. Rev. Lett.* **5**, 382 (1960); Y. S. Kim and S. Oneda, *Phys. Lett.* **8**, 83 (1964); S. V. Pepper and Y. Ueda, *Nuovo Cimento* **33**, 1614 (1964); S. Oneda, Y. S. Kim, and D. Korff, *Phys. Rev.* **136**, B1064 (1964); S. Oneda, University of Maryland report, 1964 (unpublished); K. Tanaka, *Phys. Rev.* **136**, B1813 (1964); H. J. Lipkin, *ibid.* **137**, B1561 (1965); C. Itzykson, M. Jacob, and G. Mahoux, *Nuovo Cimento Suppl.* **5**, 978 (1967); and G. V. Dass and A. N.

Kamal, *Phys. Rev. D* **1**, 1373 (1970).

<sup>12</sup>The ambiguity in the determination of the extra  $\gamma$  also shows up in previous experiments. B. Wolff lists 6 of his 13 events as being ambiguous. P. Kijewski [thesis, LBL Report No. UCRL-18433 (unpublished)] reports that probably 4 of his 27 events have incorrectly assigned  $\gamma$ 's. R. T. Edwards, E. W. Beier, W. K. Bertram, D. P. Herzo, L. J. Koester, and A. Wattenberg, *Phys. Rev. D* **5**, 2720 (1972), report that 50 out of 64 events are ambiguous.

<sup>13</sup>D. Cline, thesis, University of Wisconsin, 1964 (unpublished); B. Wolff and B. Aubert, *Phys. Lett.* **25B**, 624 (1967); P. Kijewski, thesis, LBL Report No. UCRL-18433; R. T. Edwards *et al.*, *Phys. Rev. D* **5**, 2720 (1972). While preparing this paper, R. J. Abrams, A. S. Carroll, T. F. Kycia, K. K. Li, J. Menes, D. N. Michael, P. M. Mockett, and R. Rubinstein, *Phys. Rev. Lett.* **29**, 1118 (1972), published evidence for direct emission. Their result is given in terms of the direct emission branching ratio. In terms of  $\gamma$  and  $\beta$  it can be given as  $\gamma=0$  (assuming no  $CP$  violation) and  $|\beta|=0.22 \pm 0.06$ . This is the first evidence for a definitely nonzero  $\beta$ , however, it is consistent with the limits put on  $\beta$  by this experiment. Their result was not used in Fig. 10.

<sup>14</sup>E. Fischbach and J. Smith, *Phys. Rev.* **184**, 1645 (1969).

<sup>15</sup>In fact these six events were included in part of the  $K^+ \rightarrow \pi^+ \pi^0 \gamma$  analysis.

<sup>16</sup>Assuming  $K_{\mu 3}$  rate is 3.20% as reported by Particle Data Group, *Phys. Lett.* **39B**, 1 (1972).

<sup>17</sup>Y. Fujii, *Phys. Rev. Lett.* **17**, 613 (1966).

<sup>18</sup>I. R. Lapidus, *Nuovo Cimento* **46**, 668 (1966).

<sup>19</sup>G. Oppo and S. Oneda, *Phys. Rev.* **160**, 1397 (1967).

<sup>20</sup>Particle Data Group, *Rev. Mod. Phys.* **43**, S1 (1971).

- <sup>21</sup>Gerald W. Intemann, Phys. Rev. D 2, 2630 (1970). Actually Intemann's stated range is  $1.5 \times 10^{-5}$  to  $2.1 \times 10^{-4}$ . However, this range is largely due to uncertainty in the  $d$ -wave to  $s$ -wave ratio in  $A_1$  decay. A recent experiment has shown that the  $d$ -wave contribution is less than 2%. [See J. W. Lamsa, C. R. Ezell, J. A. Gaidos, and R. B. Willmann, Nucl. Phys. B41, 388 (1972).] Assuming zero  $d$ -wave contribution one obtains the range  $(1.4 - 2.1) \times 10^{-4}$ .
- <sup>22</sup>V. S. Vanyashin, Yad. Fiz. 6, 109 (1967) [Sov. J. Nucl. Phys. 6, 79 (1968)].
- <sup>23</sup>For some other estimates of  $\epsilon$ , see N. N. Trofimenkoff, Phys. Lett. 41B, 160 (1972).
- <sup>24</sup>M. Chen, D. Cutts, P. Kijewski, R. Steining, and C. Wiegand, Phys. Rev. Lett. 20, 73 (1968).
- <sup>25</sup>M. Moshe and P. Singer, Phys. Rev. D 6, 1379 (1972).
- <sup>26</sup>See also L. M. Sehgal, Phys. Rev. D 6, 367 (1972).
- <sup>27</sup>G. Fäldt, B. Petersson, and H. Pilkuhn, Nucl. Phys. B3, 234 (1967).
- <sup>28</sup>Laurie M. Brown, Nilendra G. Deshpande, and Frank A. Costanzi, Phys. Rev. D 4, 146 (1971).
- <sup>29</sup>J. H. Klems, R. H. Hildebrand, and R. Steining, Phys. Rev. D 4, 66 (1971). For  $K^+ \rightarrow \pi^+ \nu \bar{\nu}$  see also G. D. Cable, R. H. Hildebrand, C. Y. Pang, and R. Steining, University of Chicago and Lawrence Berkeley Laboratory report, 1972 (unpublished).
- <sup>30</sup>Basically this is the method used to determine the detection efficiencies for all the rare decays. However, it is only detailed in Sec. V.
- <sup>31</sup>R. M. Weiner, Phys. Rev. Lett. 20, 396 (1968). See also E. F. Beall, *ibid.* 20, 947 (1968).
- <sup>32</sup>R. J. Oakes, Phys. Rev. Lett. 20, 1539 (1968).
- <sup>33</sup>R. J. Oakes, Phys. Rev. 183, 1520 (1969).
- <sup>34</sup>D. Cline, thesis, University of Wisconsin, 1964 (unpublished).
- <sup>35</sup>N. Christ, Phys. Rev. 176, 2086 (1968).
- <sup>36</sup>S. Okubo, Nuovo Cimento 54A, 491 (1968); R. E. Marshak, Y. W. Yang, and J. S. Rao, Phys. Rev. D 3, 1640 (1971); R. N. Mohapatra, *ibid.* 6, 2023 (1972).
- <sup>37</sup>S. K. Singh and L. Wolfenstein, Nucl. Phys. B24, 77 (1970).
- <sup>38</sup>G. Segrè, Phys. Rev. 181, 1996 (1969).
- <sup>39</sup>R. S. Willey, Phys. Rev. D 1, 2182 (1970). The  $K_L^0 \rightarrow \mu^+ \mu^-$  limit of less than  $1.9 \times 10^{-9}$  [Alan R. Clark *et al.*, Phys. Rev. Lett. 26, 1667 (1971)] has been inserted in Willey's calculation.
- <sup>40</sup>N. Cabibbo and A. Maksymowicz, Phys. Rev. 137, B438 (1965).
- <sup>41</sup>F. A. Berends, A. Donnachie, and G. C. Oades, Phys. Lett. 26B, 109 (1967).
- <sup>42</sup>C. Kacser, P. Singer, and T. N. Truong, Phys. Rev. 137, B1605 (1965).
- <sup>43</sup>See, for example, S. Weinberg, Phys. Rev. Lett. 17, 336 (1966) (soft-pion approach); A. Q. Sarker, Phys. Rev. 176, 1959 (1968) (hard-pion approach); S. N. Biswas, R. Dutt, and K. C. Gupta, Ann. Phys. (N.Y.) 52, 366 (1969) (dispersion relations); and S. N. Biswas, R. Dutt, P. Nanda, and L. K. Pandit, Phys. Rev. D 1, 1445 (1970) (chiral dynamics). This last paper contains a good summary of all the predictions of the previous theories.
- <sup>44</sup>F. Romano, P. Renton, B. Aubert, and A. M. Burbank-Lutz, Phys. Lett. 36B, 525 (1971).
- <sup>45</sup>The electron spectra were obtained from W. Singleton, who worked on the experiment reported by R. P. Ely *et al.*, Phys. Rev. 180, 1319 (1969).
- <sup>46</sup>Using  $4.86 \times 10^{-2}$  as  $K_{e3}$  branching ratio as reported by Particle Data Group, Phys. Lett. 39B, 1 (1972).
- <sup>47</sup>F. A. Berends, A. Donnachie, and G. C. Oades, Nucl. Phys. B3, 569 (1967). Their  $\tilde{f}$  corresponds to the real part of  $f_1$  and their value assuming constant form factors is used.
- <sup>48</sup>R. P. Ely *et al.*, Phys. Rev. 180, 1319 (1969).
- <sup>49</sup>M. Bourquin *et al.*, Phys. Lett. 36B, 615 (1971).
- <sup>50</sup>M. G. Doncel, Phys. Lett. 32B, 623 (1970).
- <sup>51</sup>It is interesting to note that the Romano *et al.* experiment also detected the psychological factor involved in finding the third  $\gamma$ . They report the scanning efficiency for two- $\gamma$ -ray events to be  $(86 \pm 4)\%$ , while the efficiency for three- $\gamma$ -ray events drops to  $(46 \pm 10)\%$ .